HOKKAIDO UNIVERSITY

Title	Molecular genetic study on gravitropism and gravitropic growth habit of the Arabidopsis shoot
Author(s)	佐々木, 秋
Degree Grantor	北海道大学
Degree Name	博士(生命科学)
Dissertation Number	甲第11841号
Issue Date	2015-03-25
DOI	https://doi.org/10.14943/doctoral.k11841
Doc URL	https://hdl.handle.net/2115/60423
Type	doctoral thesis
File Information	Shu_Sasaki.pdf

Hokkaido University Collection of Scholarly and Academic Papers : HUSCAP

Molecular genetic study on gravitropism and gravitropic growth habit of the Arabidopsis shoot

（シロイヌナズナシュートの重力屈性及び成長習性に関する分子遺伝学的研究）

Shu Sasaki

Biosystems Science Course
Graduate School of Life Science
Hokkaido University

March 2015

Acknwoledgements

I am grateful to Dr. Tsuyoshi Nakagawa (Shimane University) for providing GATEWAY binary vector pGWBs, Mrs. Yukiko Sugisawa and Dr. Hiroo Fukuda (Tokyo University) for microarray experiments, Dr. Takeo Sato (Hokkaido University) for providing p19 vectors and technical advices for agro-infiltration and Dr. Tatsuo Kakimoto (Osaka University) and Dr. Tomonao Matsushita (Kyusyu University) for providing pSKI015 vector, the *Agrobacterium* strain GV3101 (pMP90RK) and technical advices for activation tagging. I also thank the ABRC (Ohio State University) and GABI-Kat for providing seeds of Arabidopsis thaliana T-DNA insertion mutants. I would like to thank Dr. Atsuko Sato, Dr. Masaaki K. Watahiki (Hokkaido University) for isolation of the gravitropic mutant that was used in this study. I wish to express my sincere appreciation to Dr. Kotaro Yamamoto (Hokkaido University) for his invaluable suggestion and guidance throughout the course of my research and preparation of the manuscript.

Abstract

Gravitropic response is a control of growth direction with respect to the gravity vector. Gravity sensing process starts with downward movement of amyloplasts in statocytes and subsequent physiological signaling is presumed to regulate auxin transport. Putative signaling components, *Arabidopsis LAZY1* (*AtLAZY1*) and *ALTERED RESPONSE TO GRAVITY 1* (*ARG1*) are involved in negative gravitropism (upward bending) of Arabidopsis shoots. However, little is known about relationships between them. In this study, I examined genetic interaction between *AtLAZY1* and *ARG1* using various mutants of Arabidopsis. The double mutant *atlazy1 arg1* showed synergistic loss of stem gravitropism, implicating that there are multiple pathways of gravitropic signaling. Auxin transporter genes *PIN-FORMED 3* (*PIN3*), *PIN4* and *PIN7* did not genetically interact with *AtLAZY1*. I isolated a novel mutant *dsl1* that suppressed *atlazy1* defect. *dsl1* did not suppressed defects of *sgr2* and *eal1* that were mutants of amyloplast sedimentation, suggesting that *dsl1* specifically suppresses the AtLAZY1-dependent signaling pathway. *dsl1* encoded ASL5/LBD12 transcription factor and microarray analyses revealed that secondary cell wall deposition was significantly upregulated in *dsl1*, while expression of auxin signaling components was not altered. Moreover, I found that impaired secondary cellulose biosynthesis and inhibition of cellulose biosynthesis by isoxaben treatment attenuated stem gravitropism. These results indicate that cell wall biogenesis plays an important role in AtLAZY1-dependent gravitropism of Arabidopsis stems.

To further investigate how AtLAZY1 functioned in gravitropism, we used

fluorescence microscopy to examine the subcellular localization of AtLAZY1 and its truncated proteins fused to GFP in tobacco leaves. I found that AtLAZY1 localized to the plasma membrane through the C-terminal region, indicating that the putative transmembrane domain in the N-terminal half is not required for its localization. Next, I took a biochemical approach to investigate the membrane association of AtLAZY1. Transiently expressed AtLAZY1 in transgenic Arabidopsis was fractionated in an insoluble fraction that contained membranous compartments. The AtLAZY1 protein was solubilized by a non-ionic detergent or at a high pH condition, suggesting that AtLAZY1 is a peripheral membrane protein. I also found that when expressed in tobacco the C-terminal part of AtLAZY1 co-localized with microtubules. A microtubule binding assay showed that the C-terminal half of AtLAZY1, which localized to the plasma membrane, interacted with microtubules *in vitro*. These results suggest that AtLAZY1 may function with microtubules at the periphery of the plasma membrane in the gravity signaling process.

Table of contents

Acknowledgements i

Abstract ii

Abbreviations vi

I. Introduction 1

II. Materials and methods 5

1. Plant materials and growth conditions 5

2. Plasmid construction and plant tranformation 5

3. Activation tagging screening 7

4. Shoot gravitropism assay 7

5. Microarray analysis 8

6. Agrobacterium infiltration in *Nicotiana benthamiana* 8

7. Quantitative real-time RT-PCR 9

8. Histological analysis 10

9. Purification of AtLAZY1 protein from *Escherichia coli* 11

10. Transient overexpression of AtLAZY1 protein in Arabidopsis 12

11. Microtubule cosedimentation assay 12

III. Results 14

1. Genetic interaction between gravitropism-related genes 13

1-1. Genetic interaction between gravitropism-related genes 13

1-2. Genetic interaction between *AtLAZY1* and auxin transporter genes 14

1-3. Asymmetric auxin distribution in *atlazy1* 15

2. Genetic study of a suppressor mutant of *atlazy1* 17

2-1. Isolation of *dsl1*, a suppressor mutant of *atlazy1* 17

2-2. *dsl1* is an overexpressor of *ASL5* 19

2-3. Secondary cell wall biogenesis is promoted in *dsl1* 20

2-4. Cellulose biogenesis is involved in gravitropism 21

3. Characterization of AtLAZY1 protein 22

3-1. Subcelluler localization of AtLAZY1 and its fragments 22

3-2. The carboxy-terminal AtLAZY1 fragment may bind to microtubule 23

3-3. AtLAZY1 as a peripheral membrane protein 25

IV. Discussion 26

1. AtLAZY1 and genetic pathways in stem gravitropism 26

2. Potential involvement of secondary cell wall in stem gravitropism 29

3. Characteristics of AtLAZY1 protein 32

V. References 36

VI. Tables and Figures 48

Abbreviations

AFB	ARABIDOPSIS F-BOX PROTEIN
ARF	AUXIN RESPONSE FACTOR
ARG1	ALTERED RESPONSE TO GRAVITY 1
ASL/LBD	ASYMMETRIC LEAVES 2-LIKE / LATERAL ORGAN BOUNDARY
AtLAZY1	Arabidopsis LAZY1
AXR	AUXIN RESISTANT
CESA	CELLULOSE SYNTHASE CATALYTIC SUBUNIT A
DM	n-dodecyl-β-D-maltoside
DMSO	dimethylsulfoxide
DSL1	DO-NOT-SAY LAZY 1
EAL1	ENDODERMAL AMYLOPLAST LESS 1
EMS	ethyl methanesulfonate
ER	endoplasmic reticulum
GFP	GREEN FLUORESCENT PROTEIN
GSA	gravitropism set-point angle
GUS	β-glucuronidase
HEPES	4-(2-hydroxyethyl)-1-piperazineethanesulfonic acid
IAA19/MSG2	AUXIN/INDOLE-ACETIC ACID 19 / MASSUGU2
IRX	IRREGULAR XYLEM
MAP65-1	MICROTUBULE ASSOCIATED PROTEIN 65-1
MES	2-morpholinoethanesulfonic acid
MT	microtubule

NPH	NONPHOTOTROPIC HYPOCOTYL
NST	NAC SECONDARY-WALL THICKENING
PIN	PIN-FORMED
PGP	P-GLYCOPROTEIN
RT-PCR	reverse transcription polymerase chain reaction
SDS-PAGE	sodium dodecyl sulfate polyacrylamide gel electrophoresis
SGR	SHOOT GRAVITROPISM
SHR	SHORT-ROOT
SND	SECONDARY WALL-ASSOCIATED NAC DOMAIN
TIR	TRANSPORT INHIBITOR RESISTANT
TMD	transmembrane domain
TOC75	TRANLOCON AT THE OUTER ENVELOPE MEMBRANE OF CHLOROPLASTS
VND	VASCULAR RELATED NAC DOMAIN

I. Introduction

Directional growth of shoots and roots are thought to be important for harvesting light energy from the sun and for taking up water and nutrients from the ground, respectively. When the organs are leaned from their characteristic growth angle that is called gravitropic set-point angle (GSA), they show a bending response to restore the elongating axes (Firn and Digby 1997). This response is called gravitropism which is important for plants to keep their growth directions. The biological processes in gravitropism are conceptually divided into three sequential steps: gravity perception, formation and transduction of signals in gravity perceiving cells and asymmetric cell elongation in the organs (Fukaki et al. 1996). The starch-statolith hypothesis (Sack 1991) has been accepted as a plausible explanation of how plants sense gravity. In the hypothesis, gravity perception is proposed to be accomplished through downward movement of starch-filled amyloplasts in gravity-perceiving cells (statocytes). The studies of *shoot gravitropism* (*sgr*) mutants (Fukaki et al. 1996; Fukaki et al. 1998; Hashiguchi et al. 2010; Hashiguchi et al. 2014; Kato et al. 2002; Morita et al. 2006; Nakamura et al. 2011; Tanimoto et al. 2008; Yamauchi et al. 1997; Yano et al. 2003) have evidently revealed that sedimentation of amyloplast in the endodermis is essential for the gravity perception of shoots. In the signal formation and transduction step, physical information of amyloplast displacement is converted to physiological signal in the statocytes. The “tethered” model (Baluska and Hasenstein 1997) postulates that downward movement of amyloplasts disrupts cytoskeletal organization that is anchored to plasma membrane or ER. The disruption would cause activation of mechanosensitive receptors in

plasma membrane or ER (Yoder et al. 2001). This physiological signals could be transmitted by second messengers, such as Ca^{2+} (Sinclair and Trewavas 1997), pH changes (Fasano et al. 2001) and inositol 1,4,5-tripohophate (Perera et al. 2006). Cholodny-Went hypothesis (Went and Thimann 1937) has proposed that auxin is laterally transported across the plant organs to promote asymmetric growth. Polar localization of PIN-FORMED 3 (PIN3), an auxin transporter, has been shown to change responding to gravitropic stimulus (Kleine-Vehn et al. 2010; Rakusova et al. 2011). Although these signaling molecules and genes are shown to be involved in gravitropism, how they interacts each other and how they are ordered in the actual pathway of gravity signaling are still largely unknown.

In the stem gravitropism, there are two genes which are thought as key regulators of the gravity signaling process. One of them is *ALTERED RESPONSE TO GRAVITY 1* (*ARG1*) (Sedbrook et al. 1999) that is a candidate component of the transduction apparatus for gravity signaling. *ARG1* encodes a DnaJ protein which has an actin binding coiled-coil domain in its C-terminal region. Molecular lesions in *ARG1* reduce the gravitropism, but not phototropism, in Arabidopsis root, hypocotyl (Harrison and Masson 2008a; Harrison and Masson 2008b) and stem (Kumar et al. 2008). ARG1 associates with the plasma membrane and some compartments of the endomembrane system such as the ER (Boonsirichai et al. 2003). *arg1* is defective in localization of PIN3 to the lower side of root statocytes after gravity stimulation, resulting in impaired lateral auxin translocation (Harrison and Masson 2008b).

LAZY1, which was initially isolated in rice, is the other candidate component of the signaling machinery (Li et al. 2007; Yoshihara and Iino 2007). In the rice *lazy1* mutant, gravitropism of the coleoptile and gravity-induced nastic movement of the leaves are reduced, whereas root gravitropism is not affected (Abe et al. 1994). The

rice *lazy1* mutant has defects in lateral auxin translocation in the coleoptile following gravity stimulation. The rice LAZY1 (OsLAZY1) is a protein of unknown function that has a putative nuclear localization signal and a transmembrane domain that are required for localization in the nucleus and the plasma membrane, respectively (Li et al. 2007). An Arabidopsis ortholog of *LAZY1* (*AtLAZY1*) is also required for shoot gravitropism and specifically expressed in statocyte endodermis (Sasaki , 2011). But, its role is unknown as is the case in *OsLAZY1* (Yoshihara et al. 2013).

Both *ARG1* and *AtLAZY1* are not required for amyloplast development and displacement and seem to be involved in the same transduction level of gravitropic signaling. However, the relationship between the two genes has not been addressed. If the gravity signaling is composed of a single pathway, all known factors, including AtLAZY1, ARG1 and auxin transporters, may show strong functional relationships. Genetic interactions are divided in four types: epistatic, additive, synergistic and suppressed with respect to the functional relationships, and thus they are instrumental for the dissection of the biological process (Perez-Perez et al. 2009). Here, by analyzing multiple mutants of AtLAZY1, ARG1 and auxin transporters, we investigated their genetic interactions in stem gravitropism to uncover the functional relationships among them. We found that AtLAZY1 could essentially regulate its specific pathway of gravitropism. To further investigate the AtLAZY1-dependent pathway, we isolated a novel mutant *do-not-say lazy 1* (*dsl1*), a suppressor of *atlazy1*. *dsl1* overexpressed *ASYMMTERIC LEAVES 2-LIKE 5 / LATERAL ORGAN BOUNDARY DOMAIN 12* (*ASL5/LBD12*) transcription factor and showed enhanced deposition of secondary cell wall, indicating the involvement of secondary cell wall synthesis in gravitropic pathways in inflorescence stems. We also investigated characteristics of AtLAZY1 proteins, and found that AtLAZY1 is a peripheral

membrane protein that potentially binds to microtubules. These findings strongly suggest that AtLAZY1 plays an essential role in gravitropism through which amyloplast displacement is converted to cellular signals.

II. Materials and Methods

1. Plant materials and growth conditions

All *Arabidopsis thaliana* (L) Heynh. plants were sown on half-strength Murashige-Skoog medium (MS; Murashige & Skoog 1962) containing 0.9% (w/v) agar, 1% sucrose and 0.5 mM MES (pH5.8) and grown at 22°C under continuous white light condition. *atlazy1-1* (Yoshihara et al. 2013) seeds were obtained from GABI-Kat (Bielefeld University, Germany). Seeds of *arg1-3* (Harrison and Masson 2008b), *pin1* (SALK_097144), *pin3-4* (Friml et al. 2003), *pin4-3* (Friml et al. 2002a), *pin7-2* (Friml et al. 2003), *pgp1-101*, *pgp19-101* (Lin and Wang 2005), *irx1-5* and *irx3-4* (Brown et al. 2005) were obtained from Arabidopsis Biological Resource Center (Ohio State University, USA). *atlazy1-2* and *u8* mutant was obtained by screening and map-based cloning of our EMS-mutagenized seeds. *u8* mutant harbours G to A substitution at the 5'-splicing donor site of intron 7 of *SGR2* which leads to impaired splicing and insertion of additional 42 amino acids to SGR2 protein (Kato et al. 2002). All the mutants and lines used this study were Columbia (Col-0) background.

2. Plasmid construction and plant transformation

Primers used for contstruction of each vector is shown in Table 1. For *cauliflower mosaic virus 35S promoter (p35S)::ARG1-FLAG*, the coding sequence of *ARG1* cDNA without stop codon was amplified by polymerase chain reaction (PCR).

After subcloning into pENTR/D-TOPO (Invitrogen), the inserted sequence was introduced into pGWB11 (Nakagawa et al. 2007a) by Gateway LR reaction (Invitrogen) following the manufacturer's instruction.

For *ASL5-GFP*, the coding sequence of ASL5 was amplified and subcloned into pENTR/D-TOPO (Invitrogen). The inserted sequence was introduced into pGWB5 (Nakagawa et al. 2007a). For *ASL5pro::GUS*, the 1811 bp sequence upstream from the translational start site in the genome was amplified by PCR and then subcloned into pENTR/D-TOPO (Invitrogen). The inserted sequence was introduced into pGWB3 (Nakagawa et al. 2007a).

For the AtLAZY1 and truncated fragments, each conding sequence was amplified and subcloned into pENTR/D-TOPO (Invitrogen). The inserted sequence was introduced into pGWB5 resulting in C-terminal GFP fusion proteins. The coding sequence of AtLAZY1 was prepared by amplifying genomic sequence from Arabidopsis with PCR using primers flanked with XhoI and SpeI restriction sites (LAZY1_F_XhoI and LAZY1_R_SpeI), subcloning the amplified sequence into pT7-Blue T vector (Clontech) using Mighty Mix DNA Ligation Kit (Takara) according to the manufacturers' instructions, and digesting the resultant vector with XhoI and SpeI. The obtained AtLAZY1 fragment was cloned into pTA7002 vector (Aoyama and Chua 1997).

For mRFP-MAP65-1, the coding sequence of MAP65-1 was amplified by PCR and subcloned into pENTR/D-TOPO, and then introduced into pGWB554 (Nakagawa et al. 2007b).

For plant transformation, each construct was transferred into the *Agrobacterium tumefaciens* GV3101 (pMP90) strain by electroporation. The obtained *Agrobacterium* strains were used to generate stably transformed

Arabidopsis with the floral dip method (Clough and Bent 1998).

3. Activation tagging screening

Generation of activation tagging mutants was performed using spray method (Weigel et al. 2000) with some modifications. Briefly, *Agrobacterium tumefaciens* strain GV3101 (pMP90RK) harboring the activation tagging vector pSKI015 (Weigel et al. 2000) was cultured to stationary phase in LB liquid medium with 50 mg ml^{-1} carbenicillin. Then the bacteria were centrifuged and resuspended in 2 volumes of water with 0.02% Silwet L-77 (Biomedical Science) and 5% sucrose. The suspension was sprayed into Arabidopsis inflorescences once a week over three weeks. After spraying, seeds were harvested and sown on the soil with Basta (Bayer Crop Science) at 1/6000 dilution for selection of the transformants. About 4000 transformants were screened in this study.

4. Shoot gravitropism assay

About 14-day-old seedlings on agar plates were transferred to and grown on soil. Primary inflorescence stems, which were about 12 to 15 cm in length, were reoriented to the horizontal position under either white light or in darkness at 22°C. In the case of semi-dwarf mutants such as *dsl1*, and *irx* and *pgp* mutants, observed primary stems were about 5 cm long. Time-lapse images of the plants were taken with a Nikon D5000 digital camera. Growth angles of the stems were calculated

from images with ImageJ (http://rsb.info.nih.gov/ij/).

For isoxaben treatment, the apical 10-cm-portions were cut from the 12-cm-long primary inflorescence stems and then their basal ends were immersed in 1.5 ml tubes containing half-strength MS liquid medium with 0.05% DMSO or 500 nM isoxaben (Wako). After incubation for 24 h under continuous white light at vertical position, the cuttings was reoriented to horizontal position and the time course of their growth angles were measured as described above.

5. Microarray analysis

Stem segments from the distal 3-cm part of lateral branches were ground with a pestle in liquid nitrogen and the total RNA was extracted using Trizol reagent (Invitrogen) according to the manufacturer's instructions. The RNA was further purified using RNeasy Micro Kit (Qiagen). Purified RNA were hybridized to Affymetrics Arabidopsis 1.0 ST Array, and the data were normalized using the robust multiarray average method (Irizarry et al. 2003). All other statistical analyses were performed with R software and Bioconductor packages. Genes differentially expressed between two genotypes were defined as such when the difference was more than 2-fold, using the mean of two replicates within a genotype.

6. Agrobacterium infiltration in *Nicotiana benthamiana*

For the *35Spro::ASL5-GFP* vector, the coding sequence of *ASL5* cDNA was

amplified and subcloned into pENTR/D-TOPO (Invitrogen). The *ASL5* sequence was transferred to pGWB5 (Nakagawa et al. 2007a) by Gateway LR reaction (Invitrogen). For plant transformation, each construct was transferred into the *Agrobacterium tumefaciens* GV3101 (pMP90) strain by electroporation. The resulting *Agrobacterium* strain was cultured, harvested and resuspended in infiltration buffer containing 10 mM MES-KOH (pH 5.6), 10 mM $MgCl_2$ and 150 mM acetosyringone. The GFP signals were observed with LSM510 confocal microscopy (Carl Zeiss).

7. Quantitative real-time RT-PCR

Stem segments from the distal 3-cm part of lateral branches were ground by pestles in liquid nitrogen and then the total RNA were prepared by using Total RNA Extraction Miniprep System (Viogene) according to the manufacturer's instructions. The RNA was treated with RQ1 RNase-free DNase (Promega) and reverse transcribed by using ReverTra Ace qPCR RT Kit (Toyobo) according to the manufacturer's instructions. Real-time PCR amplification was conducted with the LightCycler 480 System (Roche) using Thunderbird SYBR qPCR Mix (Toyobo). The crossing point (beginning of the PCR exponential phase) was determined for each reaction by the Second Derivative Maximum algorithm of the LightCycler software. For relative quantification, PCR efficiencies were determined for each gene as follows: Standard curves for each gene were measured using the serially diluted cDNA samples of control. Real-time PCR efficiencies were calculated from the given slopes in the LightCycler software. The relative expression ratios of the target genes

were calculated based on their efficiencies and the crossing points deviation of the treated sample versus controls, and expressed in comparison to the reference gene *ACTIN2*.

To measure the distribution of *IAA19* and *AtLAZY1* mRNA, 10-cm-long primary stems were cut at the base and their basal ends were submerged in half-strength MS liquid medium in 1.5 ml tubes for 60 min in vertical orientation under the white light. Then, the stems were reoriented 90^{o} and harvested at each time point. RNA was extracted from three 2-cm stem segments (3 cm below the apex) that were divided into upper and lower halves by a razor blade. For RNA extraction and reverse transcription, Plant Total RNA Extraction kit and ReverTra Ace qPCR RT Master Mix with gDNA Remover (Toyobo) were used according to the manufacturers' instructions. Real-time PCR was performed as described above.

8. Histological analysis

Stem segments were fixed in 3% paraformaldehyde in phosphate buffered saline. The fixed tissues were embedded in 3% agar and sectioned with Vibratome (Leica) with 60 μm thickness. For detection of lignin, stem sections were directly observed with Nikon Eclipse 90i fluorescent microscope. For cellulose detection, sections were submerged in 0.1% calcofluor white solution. The optical filter for DAPI was used for detection of fluorescence.

GUS expression in the transgenic lines was examined as described previously (Tatematsu et al. 2004) with a modification that the plants were stained at 37^{o}C for 24 h.

9. Purification of AtLAZY1 protein from *Escherichia coli*

To obtain the poly-histidine tagged AtLAZY1 and truncated proteins, their coding sequences were amplified by PCR and subcloned into pENTR/D-TOPO vector. Then they were cloned into the bacterial expression vector pDEST17 (Invitrogen) by Gateway LR reaction. The resulting vectors were introduced into *Escherichia coli* BL21 (DE3), and the cells were grown at 28°C to an OD_{600} of 0.3 in LB medium with 50 μg ml^{-1} ampicillin. Isopropyl-β-D-thiogalactopyranoside was added to a final concentration of 0.1 mM and the cells further incubated at 28°C for 3 h. The cells were harvested by centrifugation and lysed by sonication in lysis buffer containing 20 mM potassium phosphate (pH 8.0) and 500 mM NaCl. Insoluble His-FLAG-AtLAZY1 protein collected by centrifugation was resuspended in solubilization buffer (20 mM potassium phosphate (pH 8.0) containing 500 mM NaCl, 8 M urea and 20 mM imidazole). The solution was centrifuged and the resulting supernatant was loaded onto an IMAC Sepharose 6 Fast Flow (GE Healthcare) containing immobilized nickel sulfate. The proteins bound to the column was eluted by 500 mM imidazole. Purified proteins were sequentially dialyzed against 6, 3, 1 and 0 M urea containing 20 mM potassium phosphate (pH 8.0), 500 mM NaCl and 1% Triton X-100.

10. Transient overexpression of AtLAZY1 protein in Arabidopsis

For induction of AtLAZY1, four-day-old seedlings of the *pTA7002 or pTA7002-AtLAZY1* transgenic plants were treated with half-strength MS liquid medium containing 10 μM dexamethasone (Wako) for 160 min. The samples were lysed in liquid nitrogen with zirconia beads using a ShakeMaster Auto (Biomedical Science). Polyclonal anti-AtLAZY1 antibody was prepared against AtLAZY1 protein expressed and purified from *Escherichia coli*.

For examination of the solubility of AtLAZY1, five 7-day-old seedlings treated with 10 μM dexamethasone for 160 min were homogenized in 50 μl of 20 mM HEPES (pH 7.5) plus 150 mM NaCl with or without 1% n-dodecyl-β-D-maltoside (Tokyo Kasei). After incubation for 5 min on ice, the homogenates were divided into the supernatant and the pellet by centrifugation at 25,000 *g* for 10 min. Tubulin was detected using monoclonal anti-a-tubulin antibody (DM1A, Sigma Aldrich). For examination of effects of pH, the plants were homogenized in 20 mM HEPES (pH 7.5) or 0.1 M sodium bicarbonate (pH 11.5). Anti-TOC75 antibody was obtained from Agrisera.

11. Microtubule cosedimentation assay

To prepare the MT, the porcine tubulin (HTS format, Cytoskeleton) was polymerized in PME buffer (100 mM PIPES, pH 6.9, 0.5 mM $MgSO_4$, 1 mM EGTA, 20 μM taxol) with 1 mM GTP at 37^{o}C for 60 min, and then polymerized MTs were washed once with PME buffer. The C-terminal half of AtLAZY1 (0.03 mg ml^{-1}), expressed and purified from *Escherichia coli,* was incubated in PME buffer with or without 0.4 mg ml^{-1} polymerized MTs at 25^{o}C for 3 min and then centrifuged at 29,000 *g* for 10 min.

The supernatants and pellets were separated on an SDS-PAGE gel and stained with Coomassie blue.

III. Results

1. Genetic interaction between gravitropism-related genes

1-1. Genetic interaction between *AtLAZY1* and *ARG1*

As described above, ARG1 (Kumar et al. 2008) and AtLAZY1 (Yoshihara et al. 2013) are components of the subsequent gravitropic signaling pathway in inflorescence stems of Arabidopsis, since in the mutants amyloplasts still sedimented to the bottom of endodermal cells of vertical stems (Sasaki 2011), so that gravity sensing itself is not impaired. We sought to determine the genetic interaction between *ARG1* and *AtLAZY1* by analyzing their double mutant. For the genetic study, we used a nonsense allele of *AtLAZY1* (*atlazy1-2*) which showed defects in the growth habit of primary stems and lateral branches (Figure 1) as well as *atlazy1-1* reported in a previous report (Yoshihara et al. 2013). Although stem gravitropism was defective (Kumar et al. 2008), the stem growth habit of *arg1-3* was not (Figure 1). Surprisingly, we found that a double mutant of *atlazy1-2* and *arg1-3* had a very pronounced prostrate stem, which was much more severe than that of *atlazy1-2* (Figure 1). Consistent with the severe defects in growth habit, *atlazy1-2 arg1-3* showed a dramatic reduction in stem gravitropism after being subjected to reorientation (Figure 2). While *atlazy1-2 arg1-3* showed no response to reorientation, *atlazy1-2* and *arg1-3* single mutants displayed a moderate reduction in the gravitropic response to the change in the gravity vector (reorientation). We also found that *atlazy1-2 arg1-3* showed no response under long-term gravitropic stimulus,

suggesting that *atlazy1-2 arg1-3* completely lost stem gravitropism (Figure 3). In *35Spro::ARG1-FLAG* / *atlazy1-2 arg1-3* transgenic plants, the gravitropic response was restored to that of the *atlazy1-2* phenotype (Figure 2), indicating that *arg1-3* synergistically enhanced *atlazy1-2* defects, and that over-expression of *ARG1* was able to complement *arg1-3*, but was not enough to cover all of the AtLAZY1 function.

1-2. Genetic interaction between *AtLAZY1* and auxin transporter genes

Previously it has been found that some members of the family of auxin transporter proteins are involved in gravitropic responses of the hypocotyl and the root (Friml et al. 2002b; Kumar et al. 2011; Noh et al. 2003; Rakusova et al. 2011). PIN3, 4 and 7 belong to a subgroup of PIN auxin efflux facilitator family proteins and ARG1 has been shown to function in the same pathway as PIN3 in root gravitropism (Harrison and Masson 2008b). We therefore examined the genetic interaction between *AtLAZY1* and the three *PIN*s, by constructing a quadruple mutant of *PIN3*, *4*, *7* and *AtLAZY1*. The growth habit of a *pin3-4 pin4-3 pin7-2* triple mutant (*pinT*) was similar to that of wild type, except that there was greater curvature in the apical part of the lateral branches of the mutant (Figure 1). A quadruple mutant *atlazy1-2 pinT* showed a similar growth habit to *atlazy1-2,* with greater curvature of the apical part of the lateral branches, a typical feature of *pinT*. This suggested that the mutations in the three *PINs* additively affected the *atlazy1-2* phenotypes. Although the growth habit of *pinT* appeared normal, *pinT* exhibited a slower gravitropic response in the stem than that of *atlazy1-2* (Figure 4). In *atlazy1-2 pinT*, gravitropism was further slowed down, however, a weak response was observed (Figure 4 and 5). Thus we conclude that *atlazy1-2* is likely to additively enhance *pinT* defects in stem

gravitropism. We also examined the interaction between *AtLAZY1* and other auxin-transporter genes, *PIN1* (Figure 6), *PGP1* and *PGP19* (Figure 7). *atlazy1-2* additively affected both the *pin1* (SALK_097144) single mutant and the *pgp1-101 pgp19-101* double mutant. The additive interaction between *AtLAZY1* and *PINs* or *PGPs* could be interpreted as a lack of a functional relationships between them (Martienssen and Irish 1999). Alternatively, the synergistic interaction between *ARG1* and *AtLAZY1* would indicate that they are involved in essentially different pathways, but with some convergence (Perez-Perez et al. 2009). Taken together, our results suggest that PINs and PGPs are involved in a different pathway from AtLAZY1, while PIN3, 4 and 7 might act downstream of ARG1 (Harrison and Masson 2008b) as depicted in Figure 8.

1-3. Asymmetric auxin distribution in *atlazy1*

The rice (Li et al. 2007; Yoshihara and Iino 2007) and the maize (Dong et al. 2013) *lazy1* mutants are defective in lateral auxin transport. Although there is an established method for quantification of basipetal (rootward) auxin transport in Arabidopsis stems (Lewis and Muday 2009), lateral auxin transport is difficult to measure because the tissue involved is very small. To estimate lateral auxin transport in Arabidopsis stems, we measured the asymmetric expression of the auxin-responsive *IAA19 / MASSUGU 2* gene (Tatematsu et al. 2004). One hour after horizontal re-orientation, the expression level of *IAA19* was four-fold higher in the lower half than the upper half of the wild-type stem, as revealed by quantitative real-time reverse transcription polymerase chain reaction (RT-PCR) (Figure 9), while in *atlazy1-2* stem, expression of *IAA19* was symmetrical. We also examined

whether an asymmetric expression of *AtLAZY1* occurred in wild type while responding to a gravitropic stimulus, but we did not find this (Figure 9). These results suggest that AtLAZY1 is required for the formation of auxin gradients in the stem during gravitropic responses, although we were unable to identify any auxin transporters that functioned downstream of AtLAZY1.

2. Genetic study of a suppressor mutant of *atlazy1*

2-1. Isolation of *dsl1*, a suppressor mutant of *atlazy1*

To investigate the AtLAZY1-dependent pathway of gravitropic responses, we carried out a suppressor mutant screen of *atlazy1-2,* using activation tagging mutagenesis (Weigel et al. 2000). We isolated a putative suppressor mutant, *do-not-say lazy 1* (*dsl1*), that exhibited suppression of defects in GSA in *atlazy1-2* stem (Figure 10). *dsl1* showed dwarfism with short internodes, curled leaves and reduced fertility in the mature stage. A single mutant of *dsl1* also exhibited these phenotypes, suggesting that defects other than recovery of GSA control were not connected with the *atlazy1-2* mutation. We also found that the branching angle of *atlazy1-2 dsl1* was slightly greater than that of *dsl1* (Figure 10), indicating that *dsl1* mostly, but incompletely suppressed *atlazy1-2* defects.

Because the defect in gravitropism of *atlazy1* was more obvious under white light than in darkness (Figure 11), we compared gravitropism of *atlazy1-2* and *dsl1* stems under white light. When placed horizontally under white light, the primary stems of *atlazy1-2* never reoriented to the vertical direction (Figure 11). The

gravitropic response of *dsl1* and *atlazy1-2 dsl1* stems was slower than that of wild type, but ultimately their stems did grow upwards. Consistent with the phenotype of GSA of lateral shoots, gravitropism after reorientation in *atlazy1-2 dsl1* stems was a little slower than in *dsl1* single mutant stems (Figure 11). Taken together, *dsl1* almost suppressed *atlazy1-2* defects in terms of both GSA of shoots and stem gravitropism.

To examine the effect of *dsl1* on other gravitropic mutations, we introduced *dsl1* into mutants of *SGR2* or *SGR7/SHORT-ROOT* (*SHR*). *dsl1* was crossed with *sgr2-u8* (see Materials and Methods) and *endodermal amyloplast less 1* allele of *SHR* (*shr-eal1*) (Fujihira et al. 2000; Morita et al. 2007) to make double mutants between *dsl1* and *sgr2* or *shr*. Amyloplasts of *sgr2* mutants do not sediment in endodermal cells and they show reduced or no stem gravitropism (Fukaki et al. 1996; Toyota et al. 2013). The phenotype of *sgr2-u8* was similar to that of *atlazy1-2*. Alhough *sgr2-u8 dsl1* showed a small suppression of the GSA defects of *sgr2-u8* stems (Figure 12), GSA of *sgr2-u8 dsl1* was obviously more compromised than was *atlazy1-2 dsl1*. After reorientation, the rate of gravitropic response of *sgr2-u8 dsl1* was significantly less than that of *dsl1* (Figure 13). These results indicate that *sgr2-u8* was largely unsuppressed by *dsl1*. *shr-eal1* completely loses stem gravitropism because it lacks sedimentable amyloplasts in the endodermis, and we conclude that *shr-eal1* produces no stem gravitropic signals (Fujihira et al. 2000; Morita et al. 2007). Consistently, *shr-eal1 dsl1* stem showed no response to gravitropic stimuli. Furthermore, *dsl1* did not affect the GSA of *shr-eal1* (Figure 13). Together, these results suggest that amyloplast sedimentation is essential for the pathway that is modified by *dsl1*, and that *dsl1* specifically suppresses *atlazy1-2*.

2-2. *dsl1* is an overexpressor of *ASL5*

The plasmid rescue method was used to clone the flanking genomic sequence of the T-DNA insertion sites in *dsl1*; the T-DNA was then inserted 2.1 kb from the transcription initiation site of At2g30130 which encodes a putative transcription factor ASL5/LBD12 (Figure 14). Elsewhere, a mutant that overexpresses *ASL5* has been reported by Nakazawa et al. (2003); it has a small stature, epinastic leaves and reduced fertility, and looks very similar to *dsl1* (Figure 10). We measured mRNA levels of *ASL5* in *dsl1* by RT-PCR and confirmed that *ASL5* was over-expressed in the mutant (Figure 15). We conclude that *dsl1* is an overexpressor of *ASL5*. We next examined the endogenous expression pattern of *ASL5*. Gene expression data in the public domain shows that *ASL5* is mainly expressed in flowers and roots, but is hardly expressed in stems (http://bar.utoronto.ca/efp/cgi-bin/efpWeb.cgi, Figure 16). To further investigate this expression pattern, we created a transgenic Arabidopsis that harbored the *ASL5* promoter (*ASL5pro*) fused to a β-glucuronidase (GUS) reporter gene. In the shoot of *ASL5pro::GUS* transformants, the GUS activity was observed in the putative abscission zone of the flower petals and sepals (Figure 17). In the root, *ASL5* was expressed in the quiescent center and at a putative site of lateral root initiation (Figure 17). However, no GUS signal was detected in the stem, suggesting that ASL5 is not directly involved in stem gravitropism. Thus, over-expression of *ASL5* ectopically affected AtLAZY1-dependent signaling.

2-3. Secondary cell wall biogenesis is promoted in *dsl1*

Because ASL5 is a putative transcription factor (Husbands et al. 2007), we hypothesized that transcriptional changes of downstream genes would suppress *atlazy1-2* defects in the *atlazy1-2 dsl1* double mutant. In fact, we found that ASL5 protein fused to the amino-terminus of green fluorescent protein (GFP) was localized to the nucleus when it was expressed in leaf epidermal cells of *Nicotiana benthamiana* under the cauliflower mosaic virus 35S promoter (Figure 18), suggesting that ASL5 functioned as a *bona fide* transcription factor. We therefore performed microarray experiments to identify genes differentially expressed in *atlazy1-2 dsl1* compared with the *atlazy1-2* single mutant. We identified about 3000 genes whose expressions were changed more than two fold. When the expression of these genes was compared between wild type and *atlazy1-2,* there was little difference, suggesting that transcriptional restoration of genes did not occur in the *atlazy1 dsl1* double mutant, and that it was not a cause of the suppression of *dsl1*. To further investigate how *dsl1* suppressed *atlazy1*, we carried out gene ontology enrichment analysis so as to identify biological processes that were differentially regulated by the *dsl1* mutation. Interestingly, genes with the term 'secondary cell wall biogenesis' (GO:0009834) were significantly enriched in the up-regulated genes (*P* = 2.34e-23, Figure 19). These genes included known transcriptional regulators of the secondary cell wall genes, such as *NAC SECONDARY WALL THICKENING / SECONDARY WALL NAC DOMAIN* (*NST/SND*) (Mitsuda et al. 2007; Zhong et al. 2008), *MYB46* (Zhong et al. 2007), *MYB58*, *MYB63* (Zhou et al. 2009) and *MYB103* (Ohman et al. 2012). Because NST1 and NST3 have been revealed to act as master switches of fiber formation (Mitsuda et al. 2007), we examined expression of *NST1* and *NST3* by quantitative real-time RT-PCR. *NST1* and *NST3* were significantly upregulated in *dsl1*, whereas mRNA levels of master switches of vascular wall formation,

VASCULAR-RELATED NAC DOMAIN 6 (*VND6*) (Ohashi-Ito et al. 2010) and *VND7* (Yamaguchi et al. 2008) were not changed (Figure 20), suggesting that the secondary cell wall genes were specifically upregulated in *dsl1*. It should be noted that the expression of *AtLAZY1* was also up-regulated in *atlazy1-2 dsl1.* However, our *atlazy1-2* allele was a point mutation that changed the fourth codon to a stop codon (Sasaki 2011), and so the transcriptional change of *AtLAZY1* may not have been responsible for the suppression. We then carried out histological analysis to examine whether secondary cell wall biogenesis was actually promoted in *atlazy1-2 dsl1*. Consistent with the transcriptional changes, *atlazy1-2 dsl1* showed increased deposition of cellulose and lignin in interfascicular regions of the stem (Figure 21).

2-4. Cellulose biogenesis is involved in gravitropism

To examine whether cell wall biogenesis is involved in the gravitropic response, we examined the effects of isoxaben on gravitropism of stems after reorientation. Isoxaben is a specific inhibitor of the localization of cellulose synthase catalytic subunit A (CESA) to the plasma membrane (Desprez et al. 2002; Gutierrez et al. 2009; Scheible et al. 2001). The rate of gravitropism was slower in isoxaben-treated stems than in control (DMSO-treated) stems (Figure 22), suggesting that cellulose biogenesis is involved in stem gravitropism. Of the CESAs, CESA4, 7 and 8 are involved in secondary wall synthesis, while CESA1, 3 and 6 are involved in primary wall synthesis (Carroll et al. 2012). To further investigate the role of secondary cellulose biogenesis in gravitropism, mutants of secondary CESA7 and CESA8, were analysed; *irx3-4 / cesa7* and *irx1-5 / cesa8* consistently showed severe defects in stem gravitropism (Figure 23). It should be noted that the GSA of their

stems appeared to be slightly more horizontal than that of wild type (Figure 24). However, stems of *irx* mutants were less rigid and tended to show a more prostrate habit, which may account for their apparent inability to grow upright (Turner and Somerville 1997). Taken together, these data suggest that secondary cellulose biogenesis is required for gravitropism of stems.

3. Characterization of AtLAZY1 protein

3-1. Subcelluler localization of AtLAZY1 and its fragments

We first examined the subcellular localization of AtLAZY1-GFP transiently expressed in leaf epidermal cells of *N. benthamiana,* using fluorescent microscopy. In our experiments AtLAZY1-GFP did not localize to the nucleus, but only to plasma membrane (Figure 26). This localization pattern was verified by plasmolysis assays (Figure 27). These results differ from those reported by Yoshihara et al. (2013). The difference may be due to particular constructs used by the two groups. We fused AtLAZY1 to the N-terminal of GFP, whereas Yoshihara et al. inserted GFP between amino acid residues 308 and 309 of AtLAZY1. The GFP fusion of Yoshihara et al. functionally complemented the *atlazy1-1* mutant (Yoshihara et al. 2013), while our GFP fusion was not expressed in Arabidopsis, and thus its functionality remains to be examined. Although we did not observe nuclear localization of AtLAZY1-GFP, our protein was indeed localized to the plasma membrane.

To examine which sequence was responsible for this subcellular localization,

we divided the amino acid sequence of AtLAZY1 into N- and C-terminal halves (Figure 25) and each sequence was fused to the N-terminus of GFP using gateway binary vectors (Nakagawa et al. 2007a). We found that the N-terminal half of AtLAZY1 diffused throughout the cell including cytoplasmic strands and nucleus. On the other hand, the C-terminal half was restricted to the plasma membrane (Figure 26 and 27). This result was surprising because rice LAZY1 has a putative transmembrane domain (TMD) in the N-terminal half of the protein, which has been reported to be essential for plasma membrane localization (Li et al. 2007), and a homologous sequence of the domain is also found in the N-terminal half of AtLAZY1 (Figure 26). In contrast, our result suggests that the C-terminal half of AtLAZY1 is required for plasma membrane localization. Next, we further divided the C-terminal half of AtLAZY1 into three parts, based on GlobPlot analysis (http://globplot.embl.de). Two globular regions were predicted in the C-terminal half of AtLAZY1, which we named C1 and C3, and an intermediate disordered sequence between them, named C2 (Figure 25). C2C3 protein localized to the plasma membrane, and small unknown particles or vesicles were also observed in the C2C3 sample (Figure 26). By contrast, C1C2 showed more diffused localization than C2C3.

3-2. Carboxy-terminal AtLAZY1 fragment may bind to microtubule

We also examined the subcellular localization of C3. C3 did not appear to be localized to the plasma membrane (Figure 28 and 29), suggesting that both C2 and C3 were necessary for plasma membrane localization. Instead of localizing to the plasma membrane, C3 showed a fibrous distribution pattern in the cell (Figure 28), suggesting that it might bind to MTs. To investigate whether the fibrous structure

was caused by association with MTs, we co-expressed C3-GFP with MICROTUBULE ASSOCIATED PROTEIN (MAP) 65-1 (Lucas et al. 2011) fused to mRFP. These proteins colocalized well, suggesting that C3-GFP associated with MTs (Figure 28). Treatment with a MT destabilizing drug, oryzalin, abolished fibrous localization pattern of C3, confirming that the localization pattern depends on MTs (Figure 30). We also found that C3 without C-terminal 48 residues did not show the fibrous localization pattern (Figure31), indicating that C-terminal 48 amino acids, containing conserved region V, are essential for the fibrous localization pattern.

To confirm the interaction between AtLAZY1 and MTs, we performed an *in vitro* MT co-sedimentation assay (Shoji et al. 2004). Unfortunately, when separated on a SDS-PAGE gel, full-length AtLAZY1 was indistinguishable from tubulins due to similar electrophoretic mobility, and thus the amount of AtLAZY1 was difficult to measure, even when western blotting was used for more specific detection. Therefore we examined whether or not the C-terminal half, which localized to the plasma membrane *in vivo* (Figure 26), bound to MTs. The purified C-terminal half of AtLAZY1 was mixed with taxol-stabilized MTs at 25^{o}C. In the absence of MTs, the C-terminal half of AtLAZY1 partly self-aggregated, but about 30% of the protein remained in the supernatant fraction of a sample after centrifugation (Figure 32A and B). When MTs were added, however, all of the C-terminal half was fractionated in the pellet (Figure 32A and B), suggesting a significant interaction between the C-terminal half of AtLAZY1 and MTs. We also conducted this co-sedimentation assay between C3 and MTs, and found no interaction between them (data not shown). Although speculative, these results suggest that C1C2 enhances both plasma membrane localization and interaction with MTs, and that plasma membrane localization is dominantly observed in the pavement cells.

3-3. AtLAZY1 as a peripheral membrane protein

We have shown that AtLAZY1 can be localized to the plasma membrane without the putative TMD in the N-terminal half. This suggests that AtLAZY1 is likely to be a peripheral membrane protein that localizes to the membrane through protein-protein interaction or through membrane anchoring. To further investigate this localization, we generated a transgenic Arabidopsis harboring dexamethasone (dex)-inducible AtLAZY1 with no tags (Aoyama and Chua 1997), and examined its solubility in the presence of non-ionic detergent or under high pH, using an anti-AtLAZY1 antibody. After dex induction for ~3 h, AtLAZY1 was detected in the crude protein extracts (Figure 33). We then fractionated the protein extract by centrifugation to give supernatant and pellet fractions. Consistent with the membrane localization of AtLAZY1 in Figure 1B, AtLAZY1 was fractionated to the pellet, and was solubilized to the supernatant when the tissues were extracted in the presence of a non-ionic detergent, n-dodecyl-b-D-maltoside (DM) (Figure 34). AtLAZY1 association with the membrane was sensitive to alkaline carbonate buffer (pH 11.5), and a significant amount of AtLAZY1 was observed in the supernatant after extraction with the alkaline buffer (Figure 35). In contrast, in both neutral and high pH buffers a b-barrel transmembrane channel TRANSLOCON AT THE OUTER ENVELOPE MEMBRANE OF CHLOROPLASTS (TOC) 75-III (Baldwin et al. 2005) was found only in the pellet, confirming that transmembrane proteins can not be solubilized in alkaline buffer. These results suggest that AtLAZY1 is not a transmembrane protein but is a peripheral membrane protein.

IV. Discussion

1. AtLAZY1 and genetic pathways in stem gravitropism

Gravity signaling is a process in which the mechanical signal derived from change in potential energy of gravity is converted to biochemical signals in statocytes. Although amyloplasts of *atlazy1* and *oslazy1* sediment downwards in endodermis and leaf sheath pulvini, respectively, these mutants are not able to fully respond to gravity (Abe et al. 1994). Hence LAZY1 is most likely to be involved in this conversion step of gravity signaling. There seems to be the AtLAZY1-specific pathway in gravity signaling which is suppressed by *dsl1*, because *dsl1* cannot suppress defects in gravitropism mutants such as *sgr2-u8* and *shr-eal1*. *sgr2-u8* and *shr-eal1* are compromised in amyloplast sedimentation or development, thus in these mutants all pathways of the gravity signaling are likely to be compromised in them (Figure 12). This suggests that GSA control and gravitropism are composed of at least two regulatory pathways, one of which is mediated through AtLAZY1 and susceptible to *dsl1* mutation. This conclusion is consistent with our results of genetic analysis that gravitropic signaling is composed of AtLAZY1- and ARG1-mediated pathways.

Because rice LAZY1 regulates lateral auxin translocation, it has been suggested that LAZY1 regulates expression and/or activity and localization of auxin transporter proteins (Yoshihara and Iino 2007). In the microarray results, we found that expression of PINs was unchanged in *atlazy1*, indicating that transcriptional changes of auxin transporters are unlikely to be the cause of gravitropic defects of *atlazy1* (data not shown). This is consistent with a previous finding that nuclear

localization of AtLAZY1 is not necessary for its function (Yoshihara et al. 2013). Alternatively, because AtLAZY1 localizes to plasma membrane (Yoshihara et al. 2013), AtLAZY1 may function in a biological process which occurs at the periphery of the plasma membrane, such as regulation of localization or activity of auxin transporters. Indeed, we found no asymmetric expression of *IAA19* in lateral stems of *atlazy1* (Figure 9), suggesting that the function of AtLAZY1 is actually to regulate lateral auxin transport as is the case with rice LAZY1. However, our genetic analyses have revealed that known auxin transporter genes, such as *PIN1*, *PIN3*, *PIN4*, *PIN7*, *PGP1* and *PGP19* only showed an additive genetic interaction in the stem gravitropism, indicating that AtLAZY1 is involved in a different pathway from that involving PINs and PGPs (Figure 4, 6 and 7). At present, therefore, the mechanism by which *atlazy1* leads to a defective lateral gradient of auxin remains unknown.

In each mutant we examined both GSA and the gravitropic response of inflorescence stems, and found differences between these two characteristics. Stem gravitropism was severely compromised in *arg1* and *pinT*, while their GSA was more or less normal. In contrast, *atlazy1* affected GSA control more severely than the gravitropic response (Figure 1). This phenotypic difference may suggest that PIN3, 4 and 7 are more involved in gravitropic response than in GSA control which is also consistent with the above-mentioned result that AtLAZY1 is relatively independent of PIN3, 4 and 7. Because *dsl1* suppressed defects of *atlazy1*in both GSA control and in gravitropism, *dsl1* is likely to modulate an element common to both of them. Recently, auxin has been reported to specify the stem GSA value by regulating the magnitude of the antigravitropic offset component, via TIR1-dependent auxin signaling within the statocytes. Namely, mutants with altered levels of auxin such as *yucca1D*, *wei8* and *tar2*, or mutants with altered levels of auxin response such as

axr3-10, *arf10-3*, *arf16-2*, *nph4-1*, *arf19-1*, *tir1-1*, *afb4-2* and *afb5-5* induce more or les vertical GSA phenotype of lateral shoots (Roychoudhry et al. 2013). However, except of *AXR3,* we found no significant difference in the expression levels of these genes between *atlazy1-2* and *atlazy1-2 dsl1*, indicating that modulation of auxin signaling is not likely to be involved in the suppression of *atlazy1* defects by *dsl1* (Table 2). The expression of *AXR3* was, in fact, reduced in *atlazy1-2 dsl1*. However, a null allele of *AXR3*, *axr3-10,* alone does not induce altered GSA of lateral branches; *axr3-10* shows the defect only when it is combined with *arf10-3* and *arf16-2* (Roychoudhry et al. 2013). Collectively, these indicate that *AXR3* is not responsible for *atlazy1* suppression by *dsl1*.

In addition to the auxin signaling genes, *TILLER ANGLE CONTROL 1* (*TAC1*) promotes horizontal growth of lateral stems of peach and Arabidopsis (Dardick et al. 2013). It belongs to the IGT gene family that can be divided into two subfamilies, TAC1 and LAZY1, based on conservation of the C-terminal EAR-like motif that is present only in LAZY1 subfamily proteins. While AtTAC1 and AtLAZY1 show opposite effects on GSA, the expression pattern of these two genes overlaps significantly, suggesting that they have an antagonistic function in GSA control of stem, and that spatial expression of *AtTAC1* is coordinately regulated with *AtLAZY1* (Dardick et al. 2013). Hence *AtTAC1* could be involved in *atlazy1* suppression by *dsl1*. However, in *atlazy1 dsl1*, the expression level of *AtTAC1* was not changed from that in *atlazy1* (Table 3). Taken together, we conclude that the biological process which was restored by *dsl1* is neither auxin signaling, nor misregulation of *AtTAC1*.

2. Possible involvement of secondary cell wall in stem gravitropism

In *dsl1*, a transcription factor ASL5 was over-expressed by the inserted *35S* promoter. Cellulose and lignin overaccumulated in the secondary fibers of the inflorescence stem in *atlazy1 dsl1* (Figure 21), which is likely to be the cause of the restoration of the gravitropic response and normal GSA control. Cell-wall related genes including cellulose synthase genes have been shown to be down-regulated during gravitropism when whole tissue of root apexes (Kimbrough et al. 2004) or inflorescence stems (Yokoyama and Nishitani 2006) is subjected to transcriptome analyses. But, transcripts of many cellulose synthase genes are more abundant in lower flanks of rice shoot base when compared to those in upper flanks 6 h after reorientation (Hu et al. 2013). Inhibition of cellulose biosynthesis by isoxaben reduced gravitropic response of stems, and loss-of-function mutants of secondary *CESA* genes such as *irx1* and *irx3* exhibited severely attenuated gravitropism of stems (Figure 23).

Cell elongation that is promoted in the lower flank of hypocotyls or stems in the last step of gravitropism is thought to take place through function of wall-loosening proteins such as expansin and xyloglucan endotransglucosylase/hydrolase (Cosgrove 2005). Consistently, some of genes for these two classes of protein are upregulated during gravitropic response of hypocotyl of *Brassica oleracea* (Esmon et al. 2006), root (Kimbrough et al. 2004) and stem (Yokoyama and Nishitani 2006) of Arabidopsis, and shoot base of rice (Hu et al. 2013). In contrast to the wall loosening, physiological significance of de novo synthesis of cell wall is obscure in gravitropism. Recently brassinosteroid deficiency and addition of sucrose in growth media have been shown to enhance the gravitropic response of hypocotyls, and that

this is positively correlated with cell wall rigidity (Vandenbussche et al. 2011). In fact, we previously reported that gravitropic defects of hypocotyls of an auxin signaling mutant, *nph4/arf7*, was suppressed by brassinosteroid deficiency (Nakamoto et al. 2006). These findings suggest that *dsl1* suppresses *atlazy1* defects by enhanced rigidity of the thickened secondary cell wall.

The secondary cell wall is known to respond to the gravity stimulus in two ways. First, plants acquire a resistance to conditions of hypergravity by a modification of organ morphology, a phenomenon known as 'gravity resistance' (Hoson et al. 2005). It is distinguished from gravitropism by the fact that the gravity resistance requires the activity of mechanosensitive ion channels instead of amyloplasts (Soga et al. 2005). Hypergravity induces microtubule reorientation and then leads to the development of mechanical resistance (Soga et al. 2006). Mechanical load on the Arabidopsis primary stem also activates expression of the secondary cell wall genes including *CESA4* and *CESA7* (Koizumi et al. 2009) , but a gravitropic stimulation of the stems results in downregulation of the secondary wall genes, due to relief from the weight of upper part of the stem by reorientation (Yokoyama and Nishitani 2006). Thus, gravity resistance and transcriptional changes of secondary cell wall genes may not be directly involved in gravitropism. Second, responding to the gravity stimulus, tension wood is formed in trees at the upper side of stem in an auxin-independent manner (Hellgren et al. 2004), which consequently generates a strong tensile force that pulls a leaning shoot into a vertical position (Nugroho et al. 2012). Formation of tension wood can be observed by inclining young poplar plantlets for as little as 45 min, during which time genes for lignification and cellulose synthesis are upregulated (Azri et al. 2013). Interestingly, we found that expression of *GUS* under the *AtLAZY1* promoter was localized in the

upper half of lateral branch (Sasaki 2011). This pattern is similar to the site of tension wood formation. It is therefore possible that a mechanism homologous to the tension wood formation is involved in GSA control and stem gravitropism of Arabidopsis. However, we also found that *AtLAZY1* expression itself did not respond to a gravity stimulus, and did not exhibit asymmetric pattern in the stem gravitropism (Figure 9), suggesting that transcriptional change of *AtLAZY1* was not involved at least in gravitropism.

Recently, one of a class I *KNOX* gene, *BREVIPEDICELLUS* (*BP*)/*KNAT1*, has been found to play a key role in GSA control in siliques, another lateral organ of Arabidopsis (Wei et al. 2010). *BP* is expressed in the adaxial (upper) node region at the base of the pedicels, and its expression is reduced under a weak gravity stimulus obtained by the 3-D clinorotation, where pedicels grow more horizontally than do those of the *bp* loss-of-function mutants. In the 3-D clinorotated plants, the cells in the adaxial region of the pedicel and main stem junction are elongated, and the epidermal cells at the abaxial junction are shortened compared to the control plants, leading to the more horizontal growth orientation. Interestingly, ectopic expression of *AS2*, the founding member of the *ASL* gene family, reduces *BP* expression, thus resulting in horizontal growth of pedicels (Yamaguchi et al. 2012). Moreover, *bp* shows increased deposition of lignin (Mele et al. 2003). This suggests that secondary cell wall deposition might be involved in GSA control, which responds to a prolonged change in the gravity vector. It seems reasonable to speculate that secondary cell wall formation may therefore also be involved in the gravitropic response.

Involvement of cell wall and auxin in gravitropic responses isnot mutually exclusive. Cellulose deposition has been shown to be required for maintenance of

the polar localization of PIN proteins in root (Feraru et al. 2011), although a mutation of *CESA3* for the primary cell wall formation does not compromise auxin flux in the root gravitropic response. Cellulose deposition only keeps PINs to its localization site (Feraru et al. 2011), so it is possible that AtLAZY1 indirectly regulates auxin transport through cell wall deposition. It is also possible that AtLAZY1 may regulate a general cellular process, like membrane trafficking and/or cortical microtubule organization, because these occur at and near the plasma membrane, and because both are required for localization of both auxin transporters (Ambrose et al. 2013) and cellulose synthase to the plasma membrane (Gutierrez et al. 2009).

In conclusion, we have found that gravitropism is composed of multiple, and mutually interacting pathways, each of which should be mediated through either AtLAZY1 or ARG1. Further investigation into the interaction among these genes, auxin transport and cell wall biogenesis will lead to further understanding of how higher plants respond to gravity.

3. Characteristics of AtLAZY1 protein

In this study, we showed that AtLAZY1 can be solubilized by detergent or high pH treatment, indicating that AtLAZY1 is a peripheral membrane protein, rather than a transmembrane protein. This is consistent with the fact that plasma membrane localization of AtLAZY1 does not requires a putative TMD in the N-terminal half, although whether the putative TMD is functional or not, is still unknown. According to these results, AtLAZY1 is likely to be localized to the plasma membrane through interaction with other membrane proteins. This unknown interaction of

AtLAZY1 may be an important factor in gravity perception. Maize LAZY1 (ZmLAZY1) interacts with an IAA17 transcriptional repressor protein and a protein kinase catalytic domain (PKC) (Dong et al. 2013), although the functional significance of the interactions remains elusive. ZmLAZY1 and PKC are reported to interact on the plasma membrane, and that interaction does not require the N-terminal 100 amino acids of ZmLAZY1 (Dong et al. 2013). Consistently, we showed that the C-terminal half of AtLAZY1 contributed to the plasma membrane localization. Thus AtLAZY1 possibly localizes to the plasma membrane through interaction with PKC. However, it should be noted that ZmLAZY1 localizes to the plasma membrane via TMD in the N-terminal half. This difference might reflect the species-specific function of the *LAZY1* genes. In fact, ZmLAZY1 is involved in tassel development as well as gravitropism (Dong et al. 2013), while AtLAZY1 does not seem to be (Yoshihara et al., 2013). In contrast, LAZY1 is involved in shoot gravitropism in all the plant species so far examined (Dardick et al. 2013).

The C3 region, which bound to MTs *in planta*, contains two highly conserved sequences (IV and V in Figure 25). Unfortunately, the C-terminal half and C3 did not successfully express in Arabidopsis as well as the full-length AtLAZY1, and thus functionality of the fragments remains to be examined. However, these two sequences may be important for the MT binding of AtLAZY1. We showed that C-terminal 48 amino acids were likely to be essential for colocalization with MTs *in planta* (Figure 31). *LAZY1* belongs to the *IGT* gene family that contains *TILLER ANGLE CONTROL 1* (*TAC1*) as well as *LAZY1* genes. While LAZY1 acts positively in gravitropism, TAC1 affects gravitropism negatively, and lacks the ~40 amino acid-long C-terminal region (including region V) that is more or less conserved in LAZY1 subfamily (Dardick et al. 2013). How these structural differences contribute

to their contrasting function is poorly understood. However, although speculative, it is possible that the lack of the V sequence causes loss of the MT binding, and thus TAC1 may be able to competitively inhibit the LAZY1 function.

Why the full-length AtLAZY1 did not co-localize with MTs is an interesting question. One possibility is that the N-terminal half, or the C1 and C2 regions, negatively regulate its binding affinity for MTs. In the case of a Rho GTPase, ROP11, its plasma membrane localization and co-localization with cortical MTs is observed only when MICROTUBULE DEPLETION DOMAIN 1 (MIDD1) is co-expressed with it (Oda and Fukuda 2012). Similarly MT binding of AtLAZY1 might be derepressed when a specific interactor is co-expressed with it. AtLAZY1 expresses in endodermal cells of shoots in a natural context (Yoshihara et al. 2013), thus its subcellular localization will have to be examined in the endodermal cells. However, we have not succeeded in observation of endogenous AtLAZY1, and further challenge is required for this important problem.

In conclusion, we have demonstrated that AtLAZY1 is a peripheral membrane protein which has the potential to associate with MTs; the biological significance of this association though remains unknown. Our results and previous studies strongly indicate that interaction between plasma membrane and cytoskeleton is part of the signaling pathway in gravitropic responses. ARG1 is a peripheral membrane protein involved in gravity perception of root, hypocotyl and stem (Boonsirichai et al. 2003; Sedbrook et al. 1999; Kumar et al. 2008), and has been shown to associate with actins (Harrison and Masson 2008a). ARG1 can also be solubilized by alkaline buffer and detergents (Boonsirichai et al. 2003) similarly to AtLAZY1. Hence, AtLAZY1 appears to share some characteristics with ARG1. The ‘tethered model’ for the molecular mechanism of gravity perception hypothesizes that

amyloplast sedimentation disrupts the organization of cytoskeletons anchored to membranes. This disruption may be transmitted to the membrane, thus activating mechanosensitive channels (Volkmann and Baluska 1999). It is possible that AtLAZY1 and ARG1 are involved in this hypothetical mechanism. Moreover, MTs have been supposed to influence tropism by positioning of regulatory proteins on the plasma membrane as well as cell expansion during organ bending (Bisgrove 2008). The relationship between AtLAZY1 function and MT organization should be addressed further to elucidate the molecular mechanism of gravity signaling.

V. References

Abe, K., Takahashi, H. and Suge, H. (1994) Localization of cells containing sedimented amyloplasts in the shoots of normal and lazy rice seedlings. *Biol Sci Space* 8: 221-225.

Ambrose, C., Ruan, Y., Gardiner, J., Tamblyn, L.M., Catching, A., Kirik, V., et al. (2013) CLASP interacts with sorting nexin 1 to link microtubules and auxin transport via PIN2 recycling in Arabidopsis thaliana. *Dev Cell* 24: 649-659.

Aoyama, T. and Chua, N.H. (1997) A glucocorticoid-mediated transcriptional induction system in transgenic plants. *Plant J* 11: 605-612.

Azri, W., Ennajah, A., Nasr, Z., Woo, S.Y. and Khaldi, A. (2013) Transcriptome profiling the basal region of poplar stems during the early gravitropic response. *Biol Plant* 58: 55-63.

Baluska, F. and Hasenstein, K.H. (1997) Root cytoskeleton: its role in perception of and response to gravity. *Planta* 203: S69-78.

Bisgrove, S.R. (2008) The roles of microtubules in tropisms. *Plant Sci* 175: 747-755.

Boonsirichai, K., Sedbrook, J.C., Chen, R., Gilroy, S. and Masson, P.H. (2003) ALTERED RESPONSE TO GRAVITY is a peripheral membrane protein that modulates gravity-induced cytoplasmic alkalinization and lateral auxin transport in plant statocytes. *Plant Cell* 15: 2612-2625.

Brown, D.M., Zeef, L.A., Ellis, J., Goodacre, R. and Turner, S.R. (2005) Identification of novel genes in Arabidopsis involved in secondary cell wall formation using expression profiling and reverse genetics. *Plant Cell* 17: 2281-2295.

Carroll, A., Mansoori, N., Li, S., Lei, L., Vernhettes, S., Visser, R.G., et al. (2012)

Complexes with mixed primary and secondary cellulose synthases are functional in Arabidopsis plants. *Plant Physiol* 160: 726-737.

Clough, S.J. and Bent, A.F. (1998) Floral dip: a simplified method for Agrobacterium-mediated transformation of Arabidopsis thaliana. *Plant J* 16: 735-743.

Cosgrove, D.J. (2005) Growth of the plant cell wall. *Nat Rev Mol Cell Biol* 6: 850-861.

Dardick, C., Callahan, A., Horn, R., Ruiz, K.B., Zhebentyayeva, T., Hollender, C., et al. (2013) PpeTAC1 promotes the horizontal growth of branches in peach trees and is a member of a functionally conserved gene family found in diverse plants species. *Plant J* 75: 618-630.

Desprez, T., Vernhettes, S., Fagard, M., Refregier, G., Desnos, T., Aletti, E., et al. (2002) Resistance against herbicide isoxaben and cellulose deficiency caused by distinct mutations in same cellulose synthase isoform CESA6. *Plant Physiol* 128: 482-490.

Dong, Z., Jiang, C., Chen, X., Zhang, T., Ding, L., Song, W., et al. (2013) Maize LAZY1 mediates shoot gravitropism and inflorescence development through regulating auxin transport, auxin signaling, and light response. *Plant Physiol* 163: 1306-1322.

Esmon, C.A., Tinsley, A.G., Ljung, K., Sandberg, G., Hearne, L.B. and Liscum, E. (2006) A gradient of auxin and auxin-dependent transcription precedes tropic growth responses. *Proc Natl Acad Sci U S A* 103: 236-241.

Fasano, J.M., Swanson, S.J., Blancaflor, E.B., Dowd, P.E., Kao, T.H. and Gilroy, S. (2001) Changes in root cap pH are required for the gravity response of the Arabidopsis root. *Plant Cell* 13: 907-921.

Feraru, E., Feraru, M.I., Kleine-Vehn, J., Martiniere, A., Mouille, G., Vanneste, S., et al.

(2011) PIN polarity maintenance by the cell wall in Arabidopsis. *Curr Biol* 21: 338-343.

Firn, R.D. and Digby, J. (1997) Solving the puzzle of gravitropism--has a lost piece been found? *Planta* 203: S159-163.

Friml, J., Benkova, E., Blilou, I., Wisniewska, J., Hamann, T., Ljung, K., et al. (2002a) AtPIN4 mediates sink-driven auxin gradients and root patterning in Arabidopsis. *Cell* 108: 661-673.

Friml, J., Vieten, A., Sauer, M., Weijers, D., Schwarz, H., Hamann, T., et al. (2003) Efflux-dependent auxin gradients establish the apical-basal axis of Arabidopsis. *Nature* 426: 147-153.

Friml, J., Wisniewska, J., Benkova, E., Mendgen, K. and Palme, K. (2002b) Lateral relocation of auxin efflux regulator PIN3 mediates tropism in Arabidopsis. *Nature* 415: 806-809.

Fujihira, K., Kurata, T., Watahiki, M.K., Karahara, I. and Yamamoto, K.T. (2000) An agravitropic mutant of Arabidopsis, *endodermal-amyloplast less 1*, that lacks amyloplasts in hypocotyl endodermal cell layer. *Plant Cell Physiol* 41: 1193-1199.

Fukaki, H., Fujisawa, H. and Tasaka, M. (1996) SGR1, SGR2, SGR3: novel genetic loci involved in shoot gravitropism in Arabidopsis thaliana. *Plant Physiol* 110: 945-955.

Fukaki, H., Wysocka-Diller, J., Kato, T., Fujisawa, H., Benfey, P.N. and Tasaka, M. (1998) Genetic evidence that the endodermis is essential for shoot gravitropism in Arabidopsis thaliana. *Plant J* 14: 425-430.

Gutierrez, R., Lindeboom, J.J., Paredez, A.R., Emons, A.M. and Ehrhardt, D.W. (2009) Arabidopsis cortical microtubules position cellulose synthase delivery to the plasma membrane and interact with cellulose synthase trafficking

compartments. *Nat Cell Biol* 11: 797-806.

Harrison, B. and Masson, P.H. (2008a) ARG1 and ARL2 form an actin-based gravity-signaling chaperone complex in root statocytes? *Plant Signal Behav* 3: 650-653.

Harrison, B.R. and Masson, P.H. (2008b) ARL2, ARG1 and PIN3 define a gravity signal transduction pathway in root statocytes. *Plant J* 53: 380-392.

Hashiguchi, Y., Niihama, M., Takahashi, T., Saito, C., Nakano, A., Tasaka, M., et al. (2010) Loss-of-function mutations of retromer large subunit genes suppress the phenotype of an Arabidopsis zig mutant that lacks Qb-SNARE VTI11. *Plant Cell* 22: 159-172.

Hashiguchi, Y., Yano, D., Nagafusa, K., Kato, T., Saito, C., Uemura, T., et al. (2014) A Unique HEAT Repeat-Containing Protein SHOOT GRAVITROPISM6 is Involved in Vacuolar Membrane Dynamics in Gravity-Sensing Cells of Arabidopsis Inflorescence Stem. *Plant Cell Physiol* 55: 811-822.

Hellgren, J.M., Olofsson, K. and Sundberg, B. (2004) Patterns of auxin distribution during gravitational induction of reaction wood in poplar and pine. *Plant Physiol* 135: 212-220.

Hoson, T., Saito, Y., Soga, K. and Wakabayashi, K. (2005) Signal perception, transduction, and response in gravity resistance. Another graviresponse in plants. *Adv Space Res* 36: 1196-1202.

Hu, L., Mei, Z., Zang, A., Chen, H., Dou, X., Jin, J., et al. (2013) Microarray analyses and comparisons of upper or lower flanks of rice shoot base preceding gravitropic bending. *PLoS One* 8: e74646.

Husbands, A., Bell, E.M., Shuai, B., Smith, H.M. and Springer, P.S. (2007) LATERAL ORGAN BOUNDARIES defines a new family of DNA-binding transcription factors

and can interact with specific bHLH proteins. *Nucleic Acids Res* 35: 6663-6671.

Irizarry, R.A., Hobbs, B., Collin, F., Beazer-Barclay, Y.D., Antonellis, K.J., Scherf, U., et al. (2003) Exploration, normalization, and summaries of high density oligonucleotide array probe level data. *Biostatistics* 4: 249-264.

Kato, T., Morita, M.T., Fukaki, H., Yamauchi, Y., Uehara, M., Niihama, M., et al. (2002) SGR2, a phospholipase-like protein, and ZIG/SGR4, a SNARE, are involved in the shoot gravitropism of Arabidopsis. *Plant Cell* 14: 33-46.

Kimbrough, J.M., Salinas-Mondragon, R., Boss, W.F., Brown, C.S. and Sederoff, H.W. (2004) The fast and transient transcriptional network of gravity and mechanical stimulation in the Arabidopsis root apex. *Plant Physiol* 136: 2790-2805.

Kleine-Vehn, J., Ding, Z., Jones, A.R., Tasaka, M., Morita, M.T. and Friml, J. (2010) Gravity-induced PIN transcytosis for polarization of auxin fluxes in gravity-sensing root cells. *Proc Natl Acad Sci U S A* 107: 22344-22349.

Koizumi, K., Yokoyama, R. and Nishitani, K. (2009) Mechanical load induces upregulation of transcripts for a set of genes implicated in secondary wall formation in the supporting tissue of Arabidopsis thaliana. *J Plant Res* 122: 651-659.

Kumar N.S., Stevens, M.H. and Kiss, J.Z. (2008) Plastid movement in statocytes of the arg1 (altered response to gravity) mutant. *Am J Bot* 95: 177-184.

Kumar, P., Millar, K.D.L. and Kiss, J.Z. (2011) Inflorescence stems of the mdr1 mutant display altered gravitropism and phototropism. *Environ Expr Bot* 70: 244-250.

Lewis, D.R. and Muday, G.K. (2009) Measurement of auxin transport in Arabidopsis thaliana. *Nat Protocol* 4: 437-451.

Li, P., Wang, Y., Qian, Q., Fu, Z., Wang, M., Zeng, D., et al. (2007) LAZY1 controls rice shoot gravitropism through regulating polar auxin transport. *Cell Res* 17:

402-410.

Lin, R. and Wang, H. (2005) Two homologous ATP-binding cassette transporter proteins, AtMDR1 and AtPGP1, regulate Arabidopsis photomorphogenesis and root development by mediating polar auxin transport. *Plant Physiol* 138: 949-964.

Lucas, J.R., Courtney, S., Hassfurder, M., Dhingra, S., Bryant, A. and Shaw, S.L. (2011) Microtubule-associated proteins MAP65-1 and MAP65-2 positively regulate axial cell growth in etiolated Arabidopsis hypocotyls. *Plant Cell* 23: 1889-1903.

Martienssen, R. and Irish, V. (1999) Copying out our ABCs - the role of gene redundancy in interpreting genetic hierarchies. *Trends Genet* 15: 435-437.

Mele, G., Ori, N., Sato, Y. and Hake, S. (2003) The knotted1-like homeobox gene BREVIPEDICELLUS regulates cell differentiation by modulating metabolic pathways. *Genes Dev* 17: 2088-2093.

Mitsuda, N., Iwase, A., Yamamoto, H., Yoshida, M., Seki, M., Shinozaki, K., et al. (2007) NAC transcription factors, NST1 and NST3, are key regulators of the formation of secondary walls in woody tissues of Arabidopsis. *Plant Cell* 19: 270-280.

Morita, M.T., Saito, C., Nakano, A. and Tasaka, M. (2007) endodermal-amyloplast less 1 is a novel allele of SHORT-ROOT. *Adv Space Res* 39: 1127-1133.

Morita, M.T., Sakaguchi, K., Kiyose, S., Taira, K., Kato, T., Nakamura, M., et al. (2006) A C2H2-type zinc finger protein, SGR5, is involved in early events of gravitropism in Arabidopsis inflorescence stems. *Plant J* 47: 619-628.

Murashige, T. and Skoog, F. (1962) A revised medium for rapid growth and bio assays with tobacco tissue cultures. *Physiol Plant* 15: 473-497.

Nakagawa, T., Kurose, T., Hino, T., Tanaka, K., Kawamukai, M., Niwa, Y., et al.

(2007a) Development of series of gateway binary vectors, pGWBs, for realizing efficient construction of fusion genes for plant transformation. *J Biosci Bioeng* 104: 34-41.

Nakagawa, T., Suzuki, T., Murata, S., Nakamura, S., Hino, T., Maeo, K., et al. (2007b) Improved Gateway binary vectors: high-performance vectors for creation of fusion constructs in transgenic analysis of plants. *Biosci Biotechnol Biochem* 71: 2095-2100.

Nakamoto, D., Ikeura, A., Asami, T. and Yamamoto, K.T. (2006) Inhibition of brassinosteroid biosynthesis by either a *dwarf4* mutation or a brassinosteroid biosynthesis inhibitor rescues defects in tropic responses of hypocotyls in the arabidopsis mutant *nonphototropic hypocotyl 4*. *Plant Physiol* 141: 456-464.

Nakamura, M., Toyota, M., Tasaka, M. and Morita, M.T. (2011) An Arabidopsis E3 ligase, SHOOT GRAVITROPISM9, modulates the interaction between statoliths and F-actin in gravity sensing. *Plant Cell* 23: 1830-1848.

Nakazawa, M., Ichikawa, T., Ishikawa, A., Kobayashi, H., Tsuhara, Y., Kawashima, M., et al. (2003) Activation tagging, a novel tool to dissect the functions of a gene family. *Plant J* 34: 741-750.

Noh, B., Bandyopadhyay, A., Peer, W.A., Spalding, E.P. and Murphy, A.S. (2003) Enhanced gravi- and phototropism in plant mdr mutants mislocalizing the auxin efflux protein PIN1. *Nature* 423: 999-1002.

Nugroho, W.D., Yamagishi, Y., Nakaba, S., Fukuhara, S., Begum, S., Marsoem, S.N., et al. (2012) Gibberellin is required for the formation of tension wood and stem gravitropism in Acacia mangium seedlings. *Ann Bot* 110: 887-895.

Oda, Y. and Fukuda, H. (2012) Initiation of Cell Wall Pattern by a Rho- and Microtubule-Driven Symmetry Breaking. *Science* 337: 1333-1336.

Ohashi-Ito, K., Oda, Y. and Fukuda, H. (2010) Arabidopsis VASCULAR-RELATED NAC-DOMAIN6 directly regulates the genes that govern programmed cell death and secondary wall formation during xylem differentiation. *Plant Cell* 22: 3461-3473.

Ohman, D., Demedts, B., Kumar, M., Gerber, L., Gorzsas, A., Goeminne, G., et al. (2012) MYB103 is required for FERULATE-5-HYDROXYLASE expression and syringyl lignin biosynthesis in Arabidopsis stems. *Plant J* 73: 63-76.

Perera, I.Y., Hung, C.Y., Brady, S., Muday, G.K. and Boss, W.F. (2006) A universal role for inositol 1,4,5-trisphosphate-mediated signaling in plant gravitropism. *Plant Physiol* 140: 746-760.

Perez-Perez, J.M., Candela, H. and Micol, J.L. (2009) Understanding synergy in genetic interactions. *Trends Genet* 25: 368-376.

Rakusova, H., Gallego-Bartolome, J., Vanstraelen, M., Robert, H.S., Alabadi, D., Blazquez, M.A., et al. (2011) Polarization of PIN3-dependent auxin transport for hypocotyl gravitropic response in Arabidopsis thaliana. *Plant J* 67: 817-826.

Roychoudhry, S., Del Bianco, M., Kieffer, M. and Kepinski, S. (2013) Auxin controls gravitropic setpoint angle in higher plant lateral branches. *Curr Biol* 23: 1497-1504.

Sack, F.D. (1991) Plant gravity sensing. *Int Rev Cytol* 127: 193-252.

Sasaki, S. (2011) Identification and characterization of a light-dependent gravitropism mutant of Arabidopsis, *lazy1*. Master's thesis, Graduate School of Life Science, Hokkaido University

Scheible, W.R., Eshed, R., Richmond, T., Delmer, D. and Somerville, C. (2001) Modifications of cellulose synthase confer resistance to isoxaben and thiazolidinone herbicides in Arabidopsis Ixr1 mutants. *Proc Natl Acad Sci U S A*

98: 10079-10084.

Sedbrook, J.C., Chen, R. and Masson, P.H. (1999) ARG1 (altered response to gravity) encodes a DnaJ-like protein that potentially interacts with the cytoskeleton. *Proc Natl Acad Sci U S A* 96: 1140-1145.

Shoji, T., Narita, N.N., Hayashi, K., Asada, J., Hamada, T., Sonobe, S., et al. (2004) Plant-specific microtubule-associated protein SPIRAL2 is required for anisotropic growth in arabidopsis. *Plant Physiol* 136: 3933-3944.

Sinclair, W. and Trewavas, A.J. (1997) Calcium in gravitropism. A re-examination. *Planta* 203: S85-90.

Soga, K., Wakabayashi, K., Kamisaka, S. and Hoson, T. (2005) Mechanoreceptors rather than sedimentable amyloplasts perceive the gravity signal in hypergravity-induced inhibition of root growth in azuki bean. *Functional Plant Biol* 32: 175.

Soga, K., Wakabayashi, K., Kamisaka, S. and Hoson, T. (2006) Hypergravity induces reorientation of cortical microtubules and modifies growth anisotropy in azuki bean epicotyls. *Planta* 224: 1485-1494.

Tanimoto, M., Tremblay, R. and Colasanti, J. (2008) Altered gravitropic response, amyloplast sedimentation and circumnutation in the Arabidopsis shoot gravitropism 5 mutant are associated with reduced starch levels. *Plant Mol Biol* 67: 57-69.

Tatematsu, K., Kumagai, S., Muto, H., Sato, A., Watahiki, M.K., Harper, R.M., et al. (2004) MASSUGU2 encodes Aux/IAA19, an auxin-regulated protein that functions together with the transcriptional activator NPH4/ARF7 to regulate differential growth responses of hypocotyl and formation of lateral roots in Arabidopsis thaliana. *Plant Cell* 16: 379-393.

Toyota, M., Ikeda, N., Sawai-Toyota, S., Kato, T., Gilroy, S., Tasaka, M., et al. (2013) Amyloplast displacement is necessary for gravisensing in Arabidopsis shoots as revealed by a centrifuge microscope. *Plant J* 76: 648-660.

Turner, S.R. and Somerville, C.R. (1997) Collapsed xylem phenotype of Arabidopsis identifies mutants deficient in cellulose deposition in the secondary cell wall. *Plant Cell* 9: 689-701.

Vandenbussche, F., Suslov, D., De Grauwe, L., Leroux, O., Vissenberg, K. and Van der Straeten, D. (2011) The role of brassinosteroids in shoot gravitropism. *Plant Physiol* 156: 1331-1336.

Volkmann, D. and Baluska, F. (1999) Actin cytoskeleton in plants: From transport networks to signaling networks. *Microscopy Research and Technique* 47: 135-154.

Wei, N., Tan, C., Qi, B., Zhang, Y., Xu, G. and Zheng, H. (2010) Changes in gravitational forces induce the modification of Arabidopsis thaliana silique pedicel positioning. *J Exp Bot* 61: 3875-3884.

Weigel, D., Ahn, J.H., Blazquez, M.A., Borevitz, J.O., Christensen, S.K., Fankhauser, C., et al. (2000) Activation tagging in Arabidopsis. *Plant Physiol* 122: 1003-1013.

Went, F.W. and Thimann, K.V. (1937) Phytohormones. p. xi, 294 p. The Macmillan Company, New York,.

Yamaguchi, M., Kubo, M., Fukuda, H. and Demura, T. (2008) Vascular-related NAC-DOMAIN7 is involved in the differentiation of all types of xylem vessels in Arabidopsis roots and shoots. *Plant J* 55: 652-664.

Yamaguchi, N., Yamaguchi, A., Abe, M., Wagner, D. and Komeda, Y. (2012) LEAFY controls Arabidopsis pedicel length and orientation by affecting adaxial-abaxial cell fate. *Plant J* 69: 844-856.

Yamauchi, Y., Fukaki, H., Fujisawa, H. and Tasaka, M. (1997) Mutations in the SGR4, SGR5 and SGR6 loci of Arabidopsis thaliana alter the shoot gravitropism. *Plant Cell Physiol* 38: 530-535.

Yano, D., Sato, M., Saito, C., Sato, M.H., Morita, M.T. and Tasaka, M. (2003) A SNARE complex containing SGR3/AtVAM3 and ZIG/VTI11 in gravity-sensing cells is important for Arabidopsis shoot gravitropism. *Proc Natl Acad Sci U S A* 100: 8589-8594.

Yoder, T.L., Zheng, H.Q., Todd, P. and Staehelin, L.A. (2001) Amyloplast sedimentation dynamics in maize columella cells support a new model for the gravity-sensing apparatus of roots. *Plant Physiol* 125: 1045-1060.

Yokoyama, R. and Nishitani, K. (2006) Identification and characterization of Arabidopsis thaliana genes involved in xylem secondary cell walls. *J Plant Res* 119: 189-194.

Yoshihara, T. and Iino, M. (2007) Identification of the gravitropism-related rice gene LAZY1 and elucidation of LAZY1-dependent and -independent gravity signaling pathways. *Plant Cell Physiol* 48: 678-688.

Yoshihara, T., Spalding, E.P. and Iino, M. (2013) AtLAZY1 is a signaling component required for gravitropism of the Arabidopsis thaliana inflorescence. *Plant J* 74: 267-279.

Zhong, R., Lee, C., Zhou, J., McCarthy, R.L. and Ye, Z.H. (2008) A battery of transcription factors involved in the regulation of secondary cell wall biosynthesis in Arabidopsis. *Plant Cell* 20: 2763-2782.

Zhong, R., Richardson, E.A. and Ye, Z.H. (2007) The MYB46 transcription factor is a direct target of SND1 and regulates secondary wall biosynthesis in Arabidopsis. *Plant Cell* 19: 2776-2792.

Zhou, J., Lee, C., Zhong, R. and Ye, Z.H. (2009) MYB58 and MYB63 are transcriptional activators of the lignin biosynthetic pathway during secondary cell wall formation in Arabidopsis. *Plant Cell* 21: 248-266.

Table 1. Primers used in this study

Purpose	Primer name	Sequence (5'-3')
qRT-PCR	At5g14090 qPCR F	CTACTGGCAACAGCTATTCCATTC
	At5g14090 qPCR R	ACATGCTGTTGGGTAAACCTCTT
	ACT2+S223UPL	CCGCTCTTTCTTTCCAAGC
	ACT2+AS281UPL	CCGGTACCATTGTCACACAC
	LBD12_RT_F	GATTGCATCTTCGCACCTTATTT
	LBD12_RT_F	GGTAGCTCCTGCAACATTTTGC
	SND1 qPCR F	TGCATGAGTATCGCCTCGAC
	SND1 qPCR R	ACCACCCAACCTTCTTCGTT
	NST1 qPCR F	GCTCCTCACGGCCAAAAATC
	NST1 qPCR R	CGTCTTGTGATGCTTCCCCT
	NST2 qPCR F	AGCTCGAGCCTTGGGATATT
	NST2 qPCR R	GTCGCTTTCCAAAATCCGACC
	VND6 qPCR F	CCCAACTACAATAATGCAAC
	VND6 qPCR R	GCTCATGATTAGCTGAGAA
	VND7 qPCR F	GGACGAATAAAGATCAGAACGA
	VND7 qPCR R	ATGCGGATGTATGACTTGTGTC
ARG1-FLAG	ARG1_genome_F	CACCATGAGCGCGAAAAAGCTTGAAGGTT
	ARG1_genome_R	ACCAAGCTTCTTATCAGATCCTTTTAGGTT
ASL5-GFP	LBD12_F	CACCATGGGCGGTCCCGGATCATCACC
	LBD12_R_NS	AGTCCAAAGAGATTCTTGCTTAAGAG
ASL5pro::GUS	LBD12pro_F	CACCAAATAGGGGGAGTCGGGGAG
	LBD12pro_R	CTTCTACTATGATCGTGATTACACCGG
pTA7002-AtLAZY1	LAZY1_F_XhoI	CACCCTCGAGATGAAGGTATGGTCTATATCTAAAAACC
	LAZY1_R_SpeI	GGACTAGTTTACAGTTCCAACACGAAATCTGCAAATC
Truncated AtLAZY1 constructs	At5g14090 cDNA F	CACCATGAAGTTTTGGGGCTGGAT
	LAZY1_F544	CACCATGAAGTTCCCACTCCAAGAGTATT
	LAZY1_F715	CACCATGGCTCACAAGTCCGCAAAGC
	LAZY1_F760	CACCATGATACACCCATCCTCAAGGGGC
	LAZY1_R930	ATTTGCTTTGCTGCTTTTTGGAT
	At5g14090 cDNA R	CAGTTCCAACACGAAATAGTCTTCGTC
	LAZY1_R759	CTTTTTCAGTACCTTCTTCACAAGATG
mRFP-MAP65-1	MAP65_1_Fgw	CACCATGGCAGTTACAGATACTGAAAG
	MAP65_1_Rgw	TCATGGTGAAGCTGGAACTTG

Table 2. Expression levels of GSA-related genes (Roychoudhry et al. 2013) in wild type, *atlazy1-2* and *atlazy1-2 dsl1*

Probe Set ID	WT_1	WT_2	atlazy1-2_1	atlazy1-2_2	atlazy1-2 dsl1_1	atlazy1-2 dsl1_2	Gene name	AGI number	Description
13335698	61.25	40.54	43.57	33.82	8.41	13.94	AXR3	AT1G04250.1	AUX/IAA transcriptional regulator family protein
13371602	7.15	6.56	4.47	6.77	4.71	6.73	TAR1	AT1G23320.1	tryptophan aminotransferase related 1
13357435	21.50	18.27	12.26	13.36	25.78	19.42	TAA1 (WEI8)	AT1G70560.1	tryptophan aminotransferase of Arabidopsis 1
13398247	241.02	187.25	197.91	202.03	225.42	256.36	ARF10	AT2G28350.1	auxin response factor 10
13463509	732.37	574.30	644.26	748.47	963.97	1083.35	TIR1	AT3G62980.1	F-box/RNI-like superfamily protein
13488887	52.64	144.02	162.91	157.06	199.06	104.04	AFB4	AT4G24390.1	RNI-like superfamily protein
13489035	34.02	35.09	27.54	35.21	31.57	36.09	TAR2	AT4G24670.1	tryptophan aminotransferase related 2
13491395	52.20	56.67	49.26	54.65	60.31	55.43	ARF16	AT4G30080.1	auxin response factor 16
13476571	3.28	2.45	2.35	5.43	2.81	3.22	YUC1	AT4G32540.1	Flavin-binding monooxygenase family protein
13528833	535.25	544.06	544.71	603.88	677.12	674.18	NPH4	AT5G20730.1	Transcriptional factor B3 family protein / auxin-responsive factor AUX/IAA-related
13537696	281.38	188.81	203.26	303.07	351.47	411.03	AFB5	AT5G49980.1	auxin F-box protein 5

Table 3. Expression level of *AtTAC1* in wild type, *atlazy1-2* and *atlazy1-2 dsl1*

Probe Set ID	WT_1	WT_2	atlazy1-2_1	atlazy1-2_2	atlazy1-2 dsl1_1	atlazy1-2 dsl1_2	Gene name	AGI number	Description
13405896	33.54	37.55	29.90	23.82	20.49	16.63	TAC1	AT2G46640.3	Tiller Angle Control 1

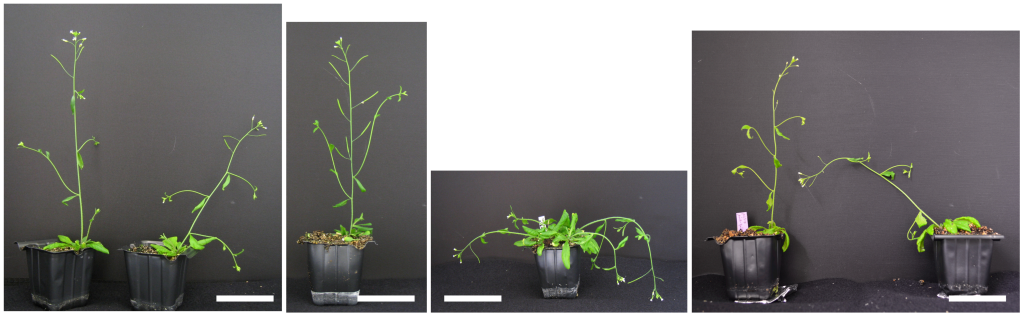


Figure 1. Morphological features and growth habit of the gravitropic mutants examined in this study. Plants were five weeks old. Bar = 5 cm.

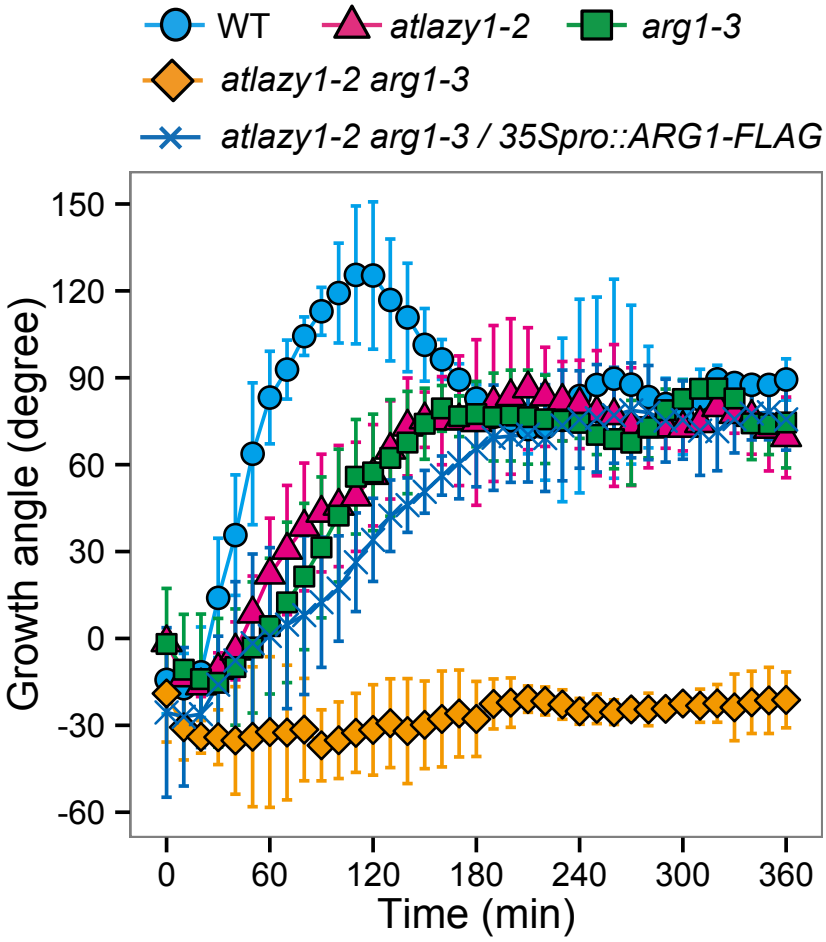


Figure 2. Time course of gravitropic response of infloresence stems of wild type (cyan circle), *atlazy1-2* (magenta triangle), *arg1-3* (green, square), *atlazy1-2 arg1-3* (yellow diamond) and *35Spro::ARG1-FLAG / atlazy1-2 arg1-3* transgenic plant (light blue cross) for molecular complementation of *arg1-3* under dark condition. The data represent mean ± SD of at least three plants.

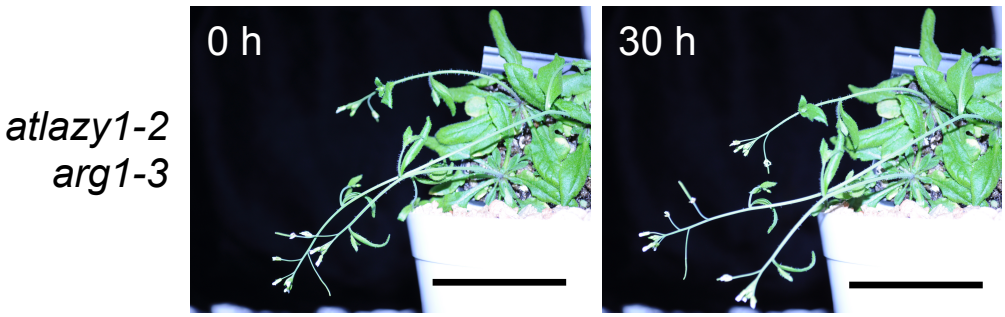


Figure 3. Gravitropism of *atlazy1-2 arg1-3* after a 30-h-long exposure to gravity stimulus under dark condition. *atlazy1-2 arg1-3* showed almost no upward bending. Bar = 5 cm.

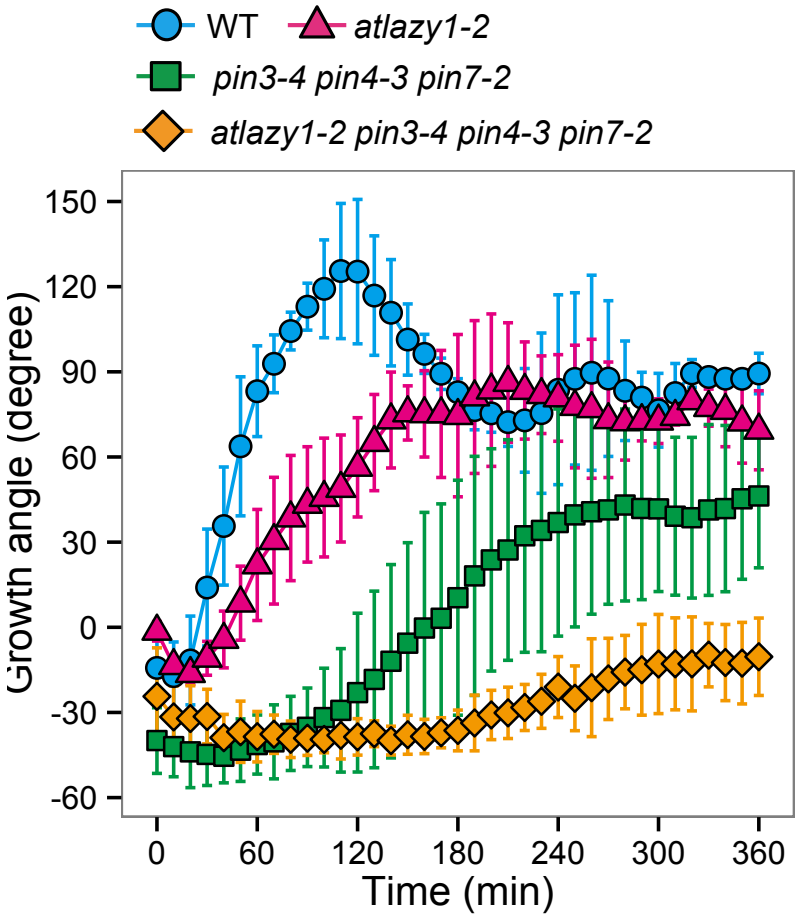


Figure 4. Time course of gravitropic response of *pin3-4 pin4-3 pin7-2* (green square) and *atlazy1-2 pin3-4 pin4-3 pin7-2* (yellow diamond) stems. Wild type and *atlazy1-2* data are the same as shown in B. The data represent mean ± SD of at least three plants.

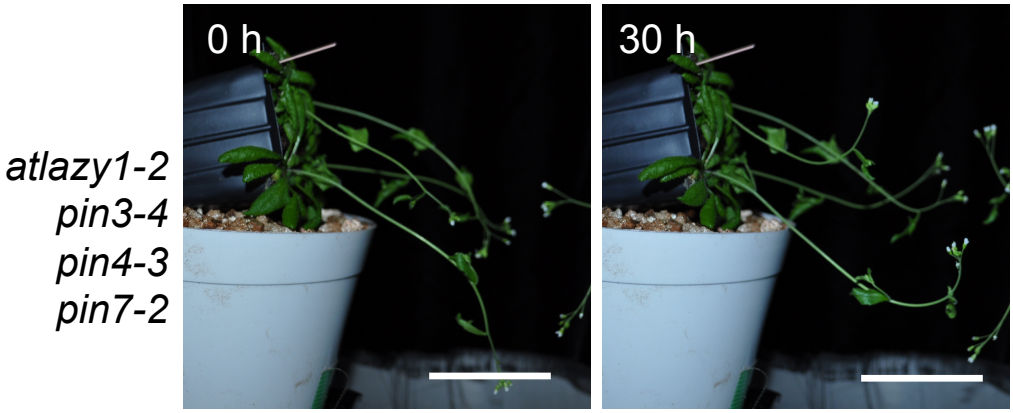


Figure 5. Gravitropism of *atlazy1-2 pinT* after a 30-h-long exposure to gravity stimulus under dark condition. *atlazy1-2 pinT* bent upward under a long-term gravitropic stimulus. Bar = 5 cm.

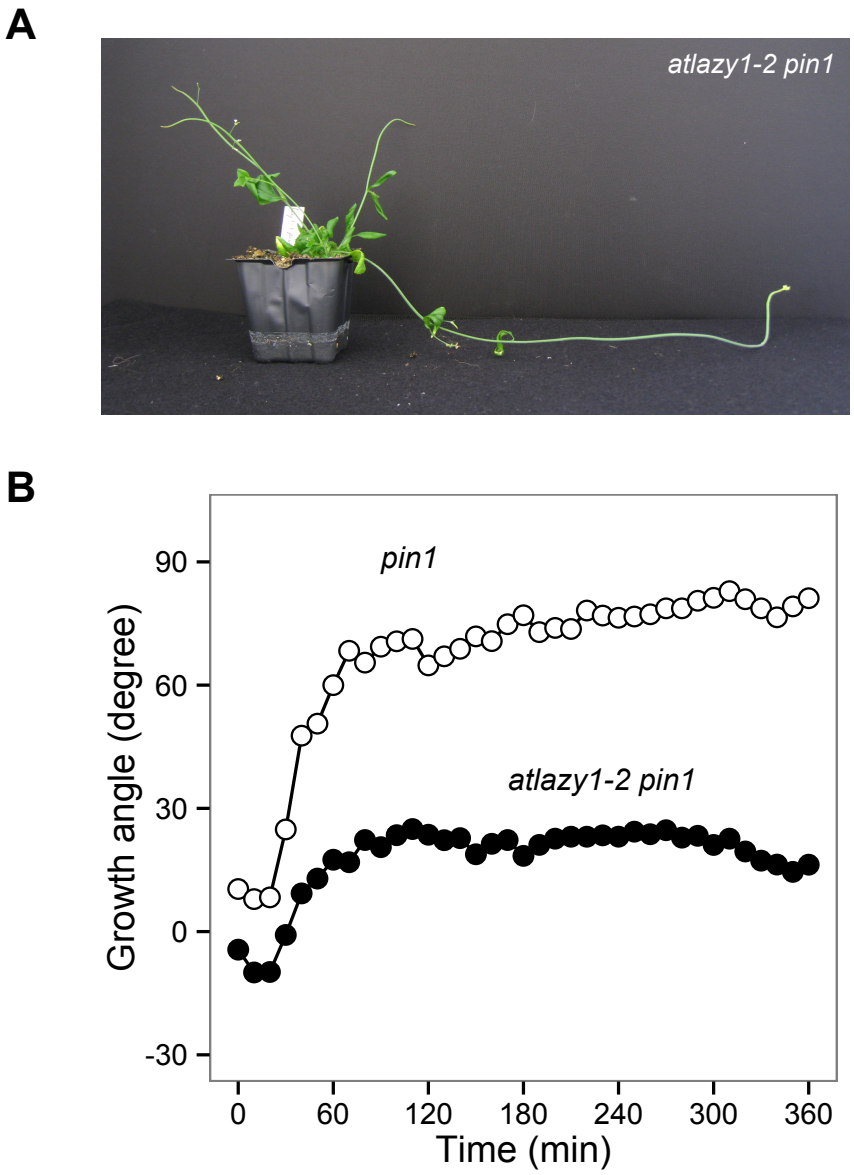


Figure 6. (A) Growth habit of *atlazy1-2 pin1.* (B) Gravitropism of inflorescence stems of *pin1* and *atlazy1-2 pin1*under white light condition.

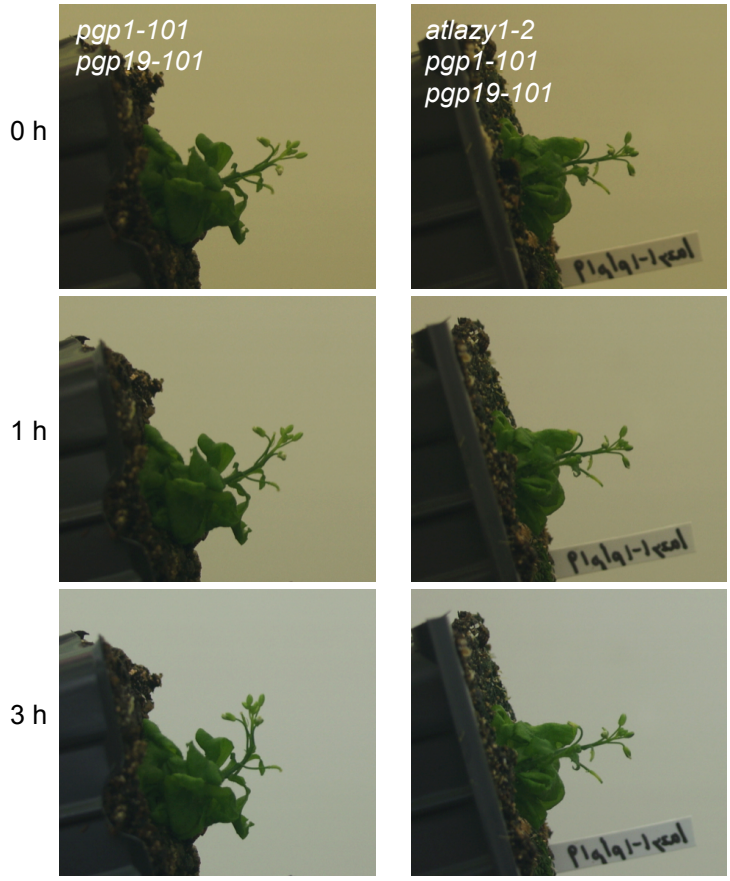


Figure 7. Gravitropism of inflorescence stems of *pgp1-101 pgp19-101* and *atlazy1-2 pgp1-101 pgp19-101* under white light condition.

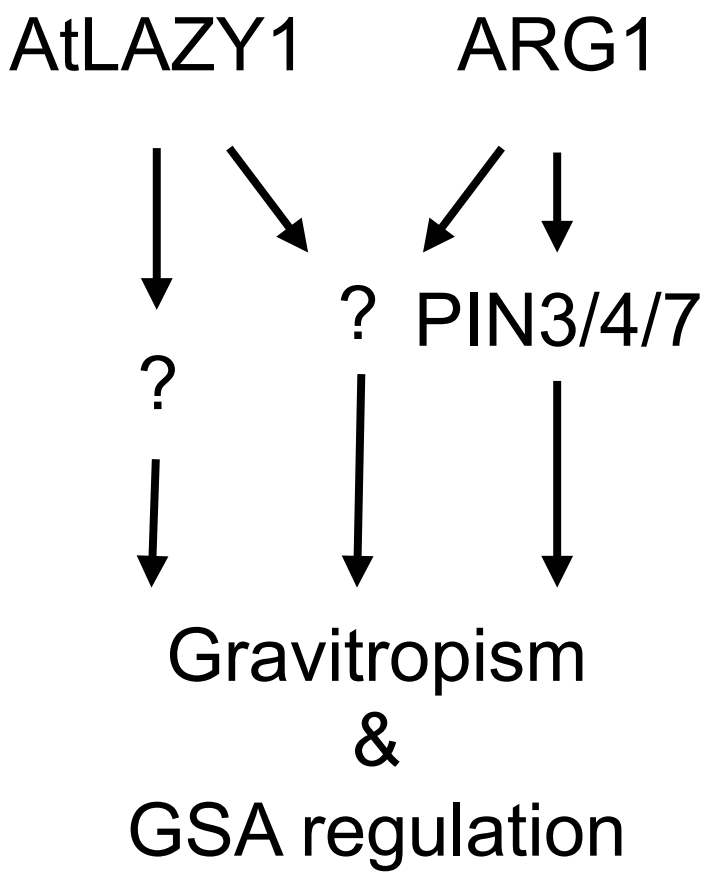


Figure 8. Schematic representation of hypothetical genetic pathways of stem gravitropism proposed in this study.

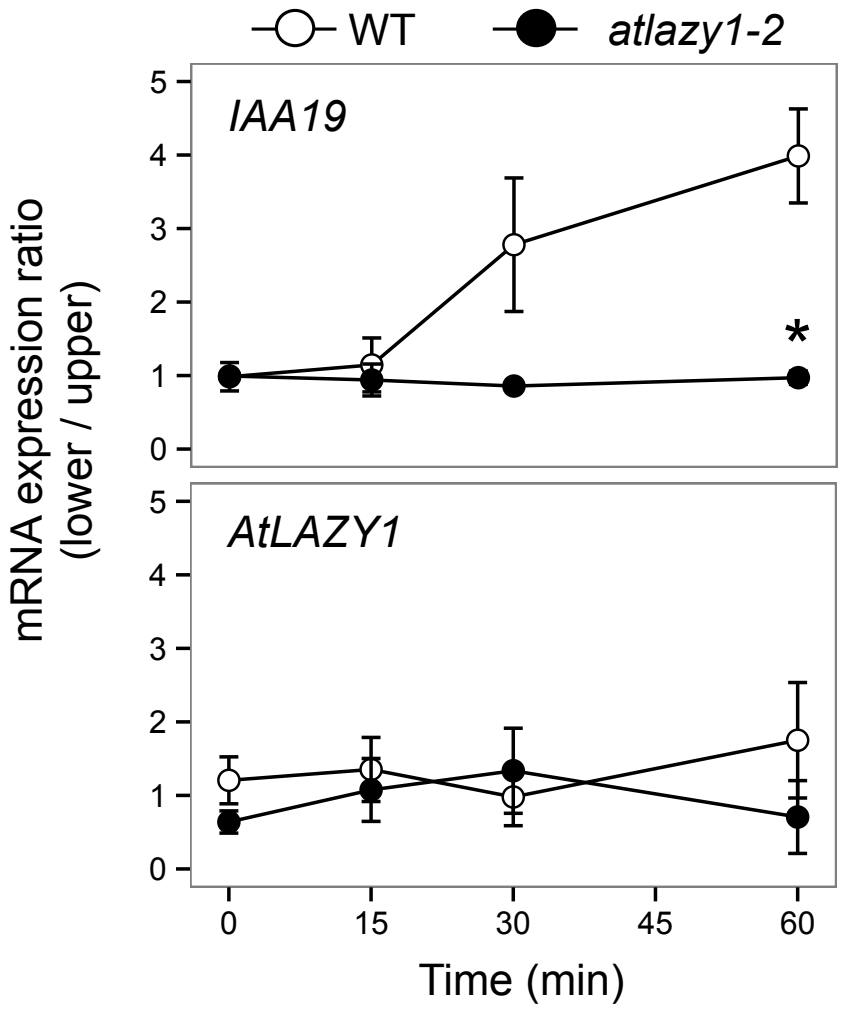


Figure 9. Time course of expression ratio between upper and lower halves of inflorescence stem under the gravity stimulus. Stems was reoriented horizontally and they were divided into upper and lower halves in each time point. The gene expression was quantified by real-time RT-PCR. A primary auxin response gene, *IAA19*, was differentialy expressed in lower halves in the wild type (open circle), whereas differential expression was not observed in *atlazy1-2* (closed circle). The data represent mean ± SD of three samples. Asterisk represents statistical significance ($p < 0.05$, Student's *t*-test)



Figure 10. Growth habit of about five-week-old plants of the *atlazy1-2 dsl1* double mutant.

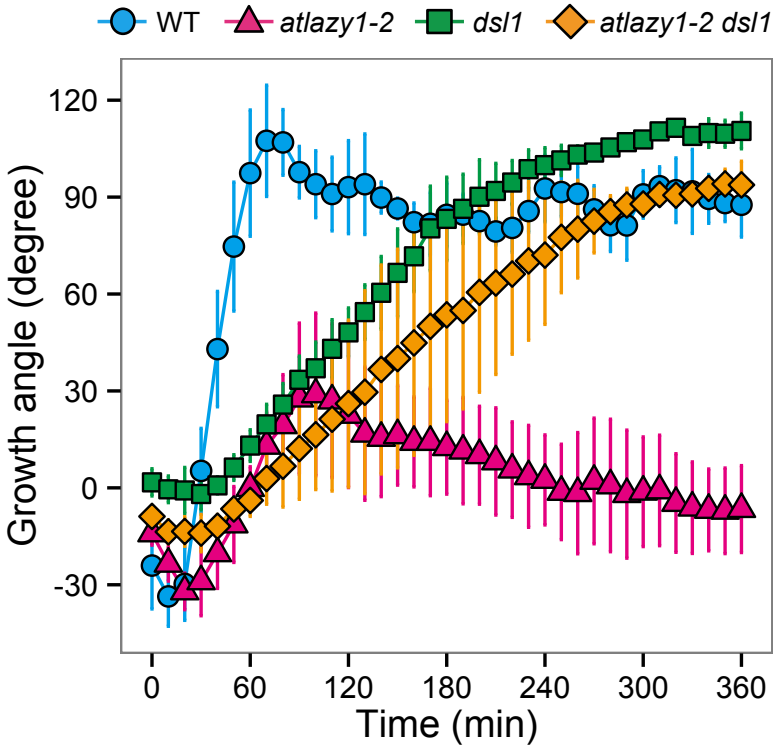


Figure 11. Time course of gravitropic response of infloresence stems of wild type (cyan circle), *atlazy1-2* (magenta triangle), *dsl1* (green square) and *atlazy1-2 dsl1* (yellow diamond) under white light condition. The data represent mean ± SD of at least three plants.



Figure 12. Growth habit of *sgr2-u8* (Sato et al. 2014), *shr-eal1* (Fujihira et al. 2000) , *atlazy1-2 dsl1*, *sgr2-u8 dsl1* and *shr-eal1 dsl1*.

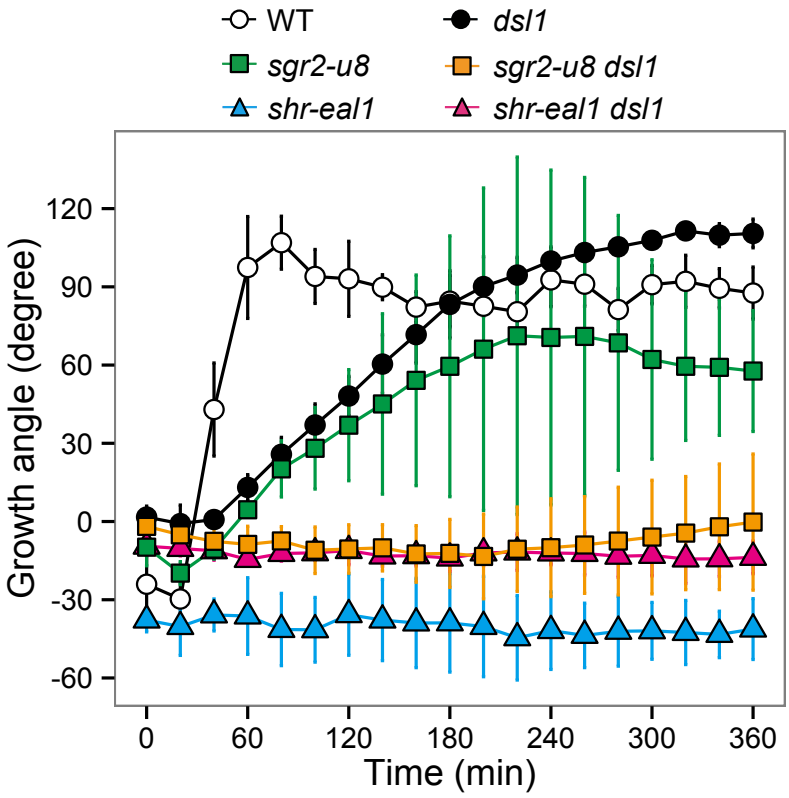


Figure 13. Time course of gravitropic response of wild type (open circle), *dsl1* (closed circle), *sgr2-u8* (green square), *sgr2-u8 dsl1* (orangle square), *shr-eal1* (cyan triangle) and *shr-eal1 dsl1* (magenta triangle). Data of the wild type and *dsl1* are the same as in Figure 11. The data represent mean ± SD of at least three plants.

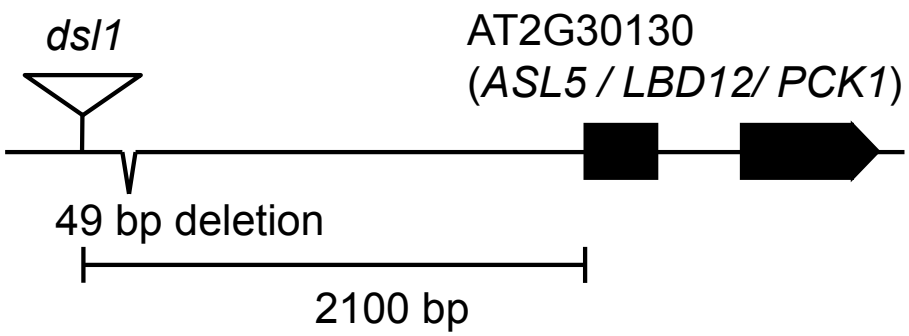


Figure 14. Schematic representation of *dsl1* allele.

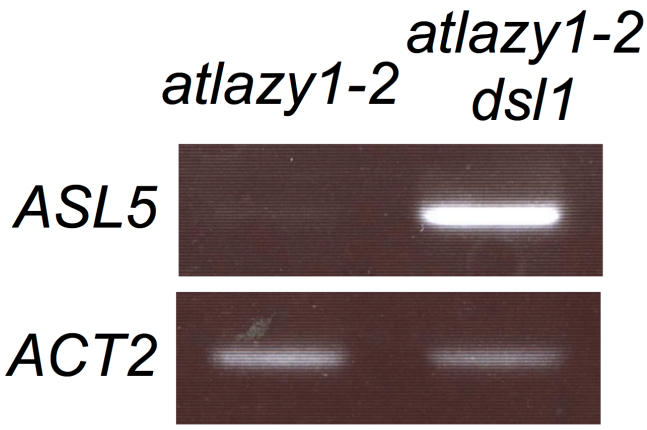


Figure 15. Semiquantitative RT-PCR analysis of mRNA extracted from *atlazy1-2* and *atlazy1-2 dsl1*. *ACTIN 2* was used as a control.

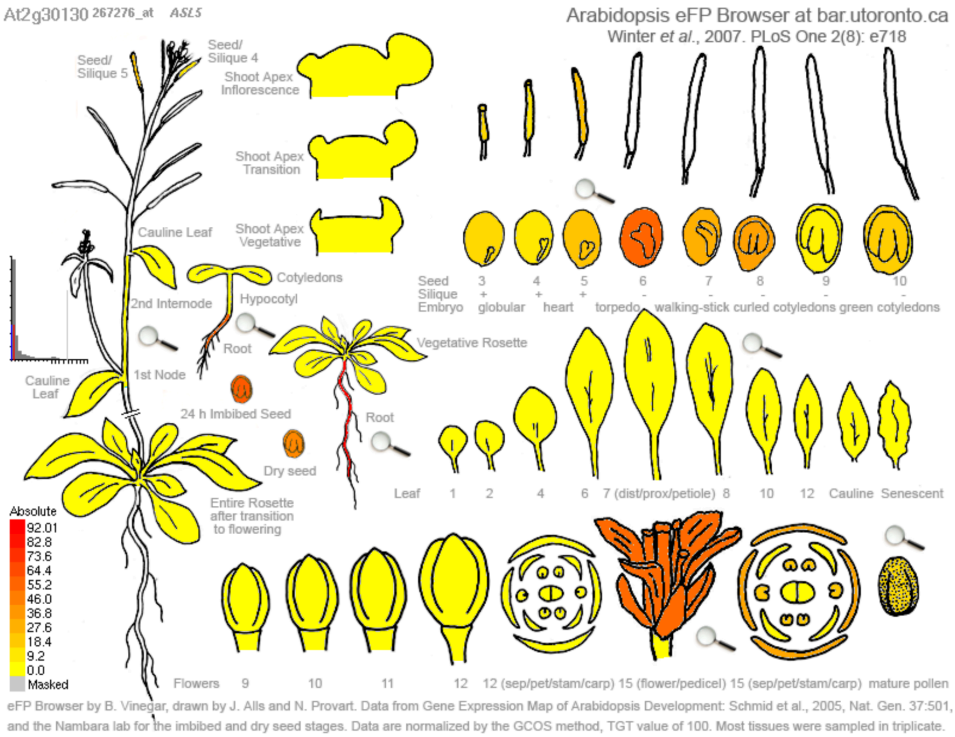
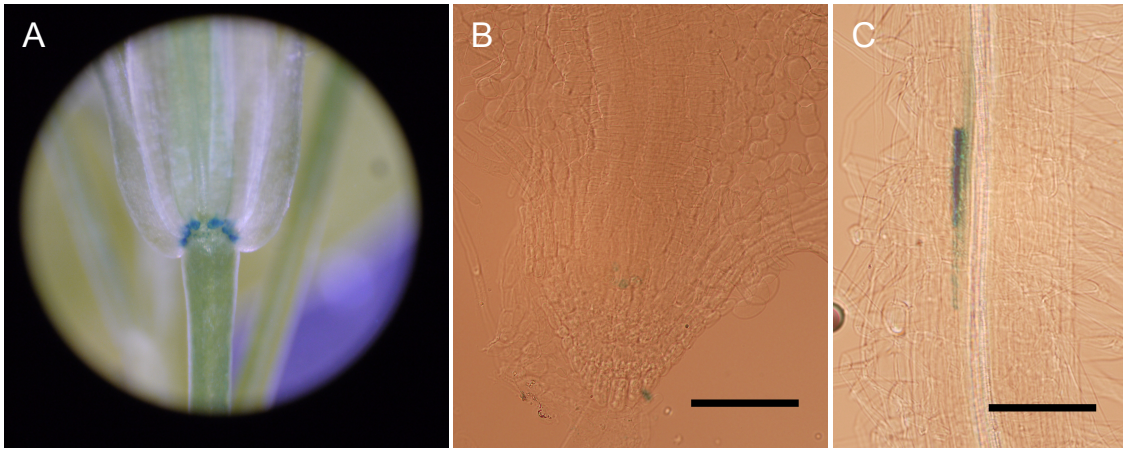


Figure 16. The expression pattern of *ASL5* gene shown in Arabidopsis eFP Browser (http://bar.utoronto.ca/efp/cgi-bin/efpWeb.cgi).



Figurer 17. (A) GUS staining of a flower of the *ASL5pro::GUS* transgenic plant. The GUS signal was only detected in the putative abscission zone of flower petals and sepals. (B) and (C) GUS staining of a root of *ASL5pro::GUS*. The GUS signal was detected in the quiescent centre of the root apex (B) and a putative site of lateral root initiation (C). Bar = 100 μm.

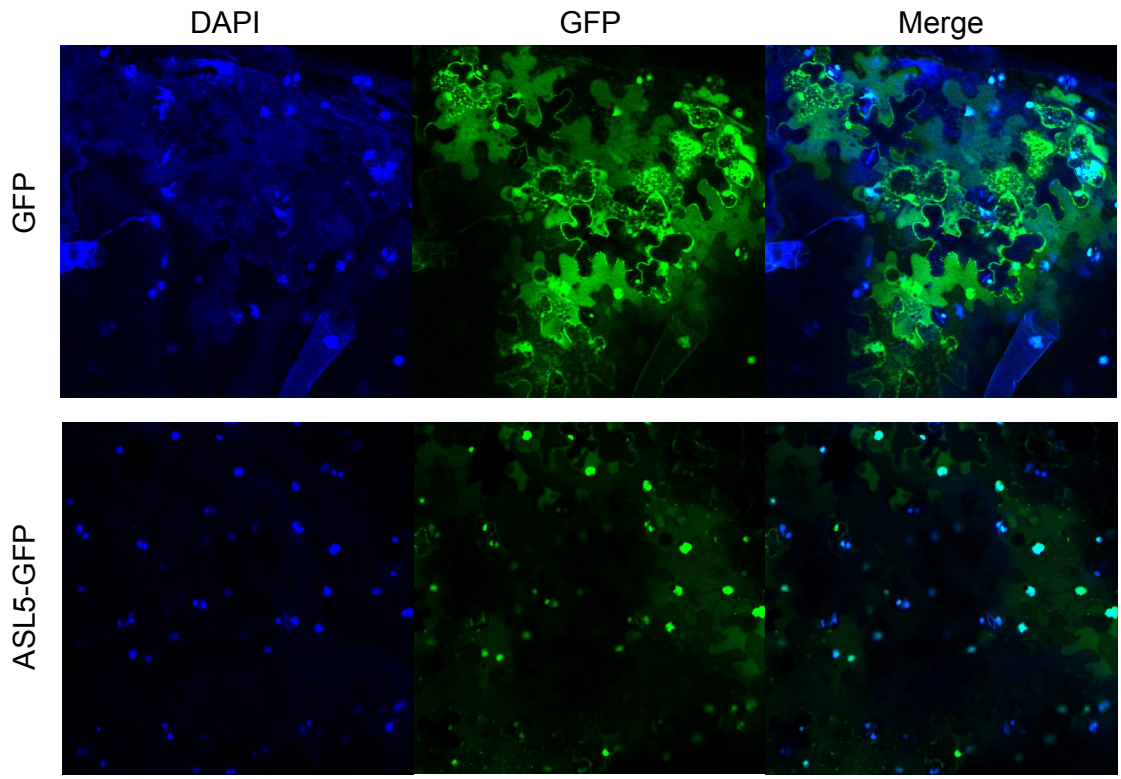


Figure 18. Subcellular localization of ASL5-GFP protein in leaf epidermal cells of *N. benthamiana*. Nuclei were stained with DAPI. ASL5-GFP was colocalized with DAPI signals.

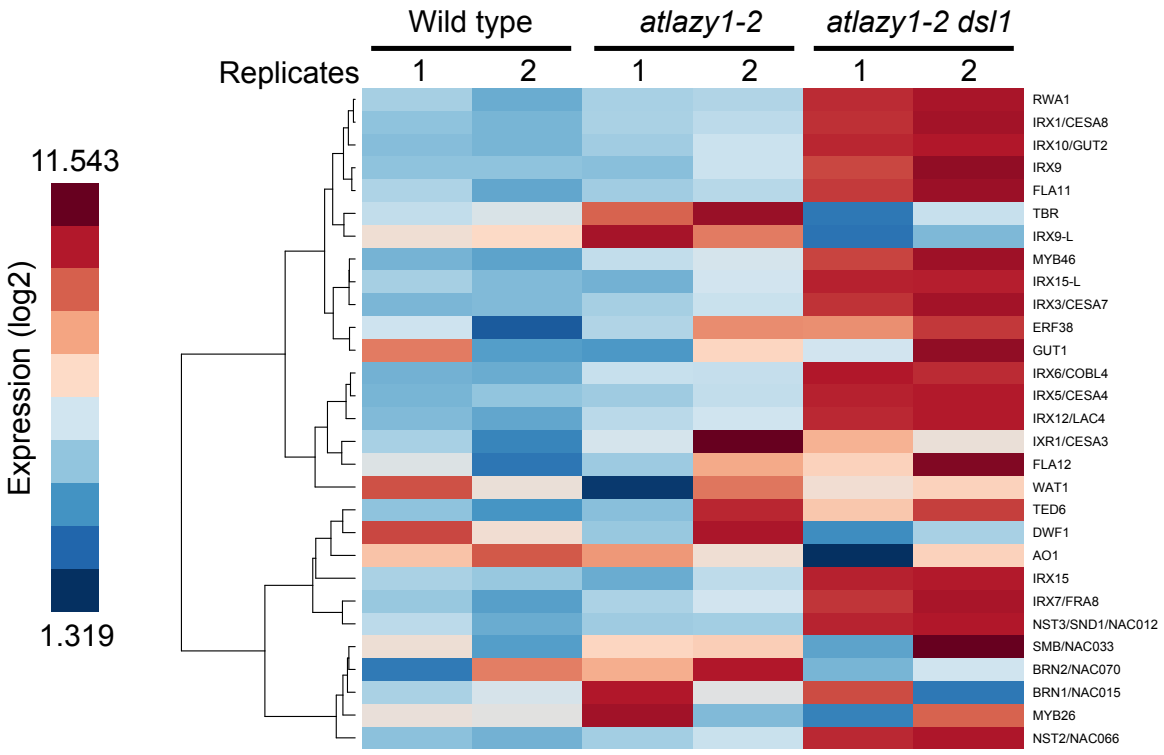


Figure 19. Heatmap of the gene expression of wild type, *atlazy1-2* and *atlazy1-2 dsl1*. The heatmap represents expression of genes in the GO category 'GO:0009834—secondary cell wall biogenesis'. The heat map and the hierarchical clustering dendrogram on the left side were generated using the R-software package.

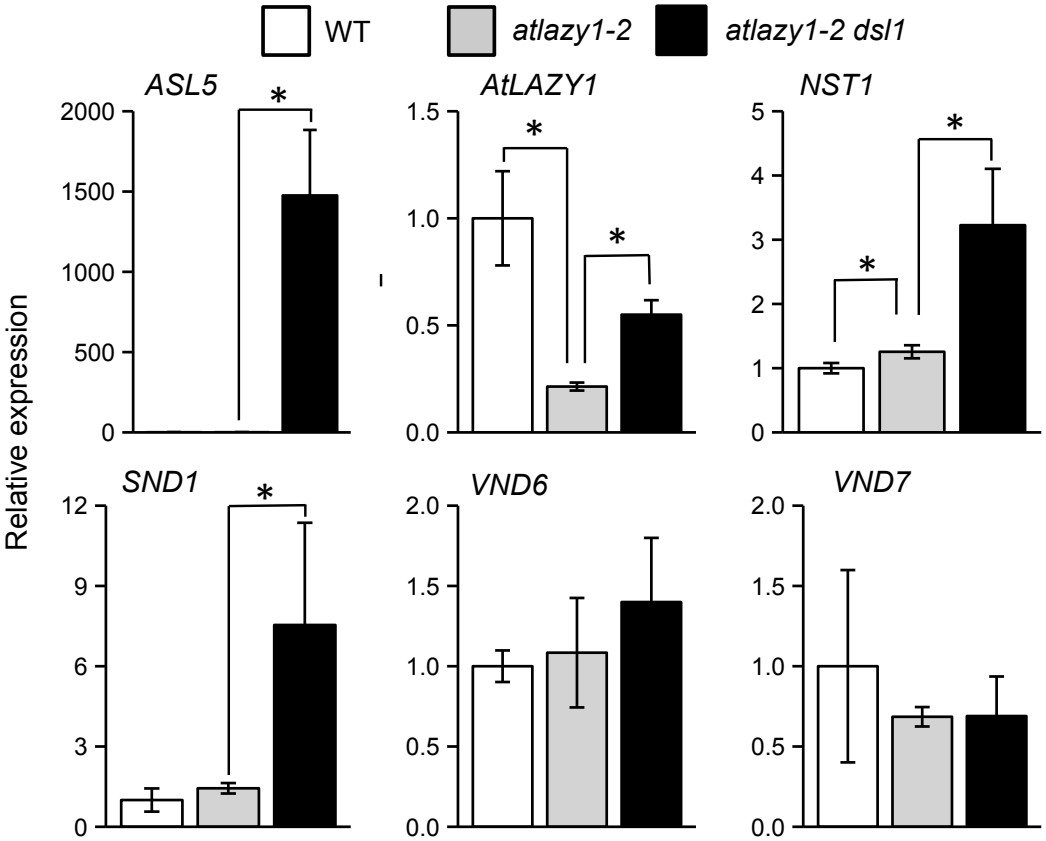


Figure 20. Quantitative real-time RT-PCR analyses of mRNA extracted from *atlazy1* and *atlazy1 dsl1.* Data represent mean ± SD of four biological replicates. Asterisks represent statistical significance ($p < 0.05$, Student's *t*-test).

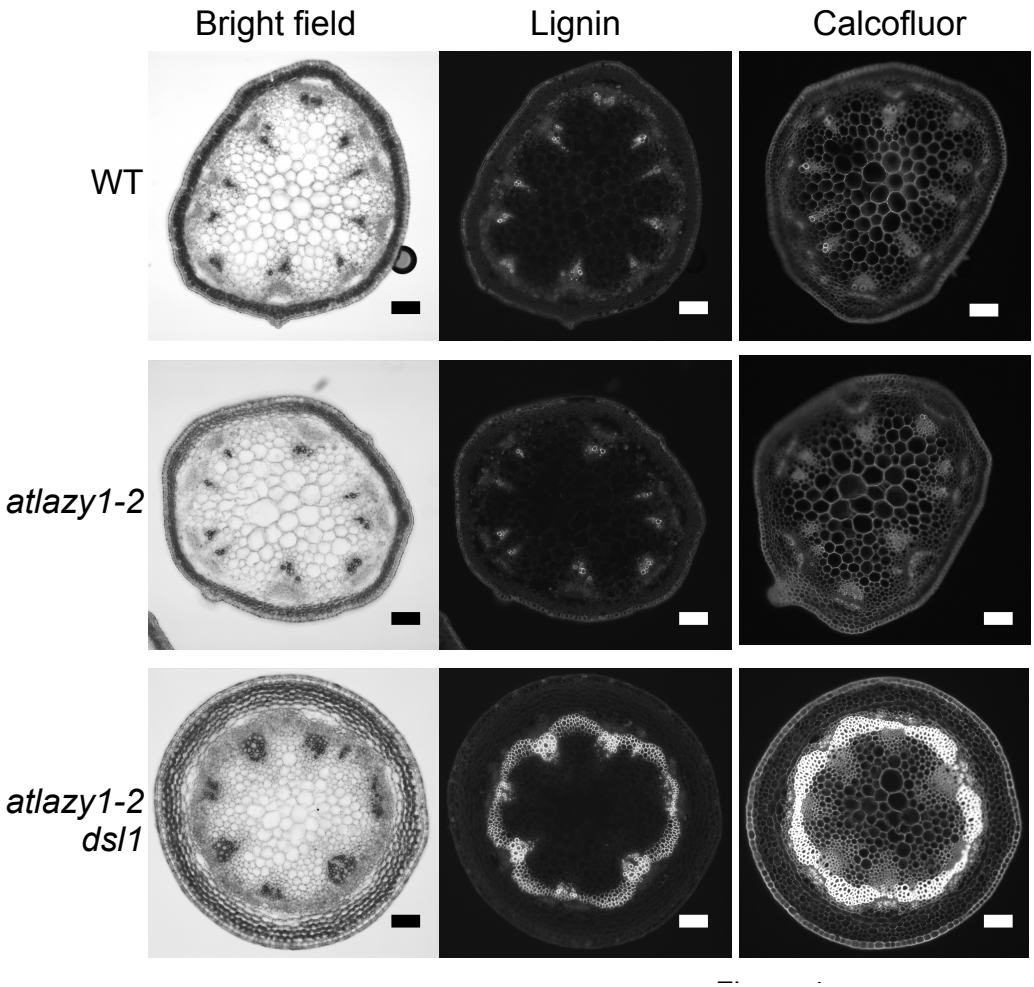


Figure 21. Cross sections of the distal 2-cm part of primary inflorescence stems. Bright-field and fluorescent images of the same sections are shown in the left and middle column, respectively. The fluorescent images represent autofluorescence of lignin. The right panels show stem sections stained with Calcofluor White to visualize cellulose fibers. Scale bars = 100 μm.

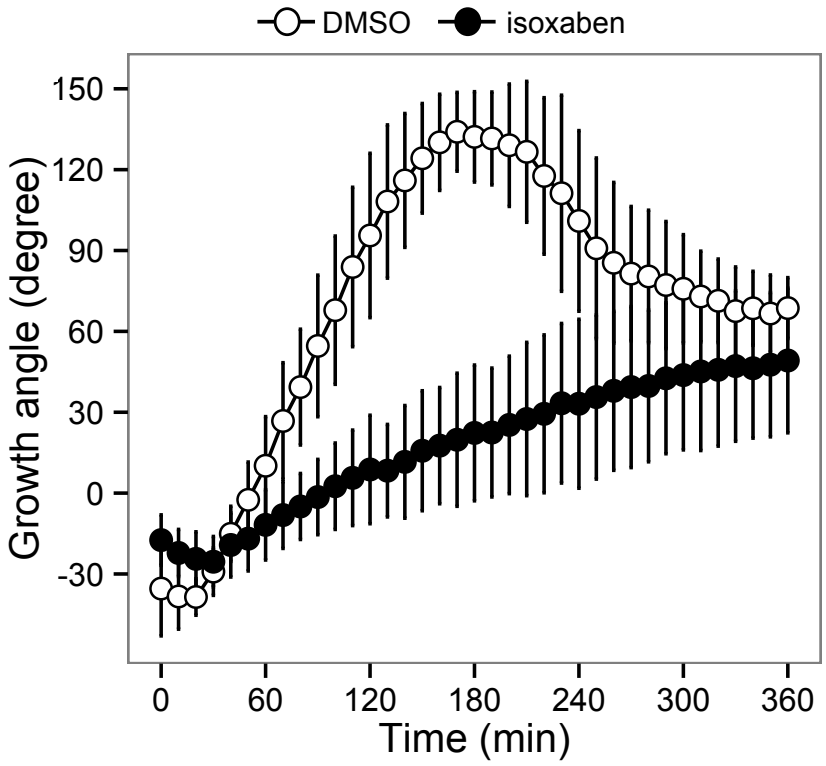


Figure 22. Time course of gravitropism of stem segments treated with mock (DMSO; open circle) and 500 nM isoxaben (closed circle). At least five stems were measured in each treatment.

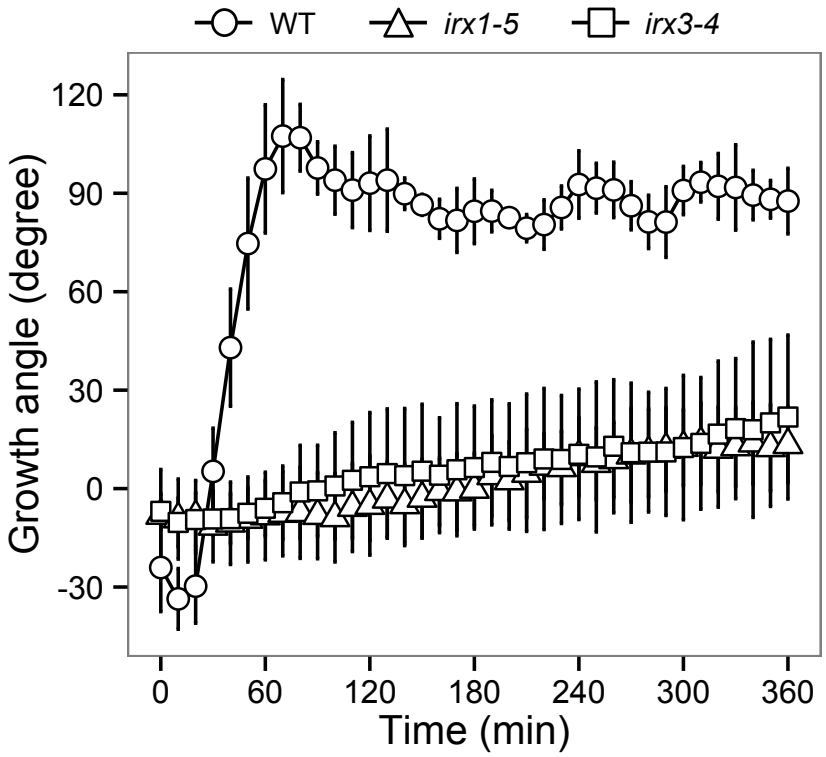


Figure 23. Time course of gravitropism of wild type (circle), *irx1-5* (triangle) and *irx3-4* (square) stems. Three individuals were measured in each genotype.



Figure 24. Growth habit of 2-month-old seedlings of *irx1-5* grown in a 5.5-cm-square pot.

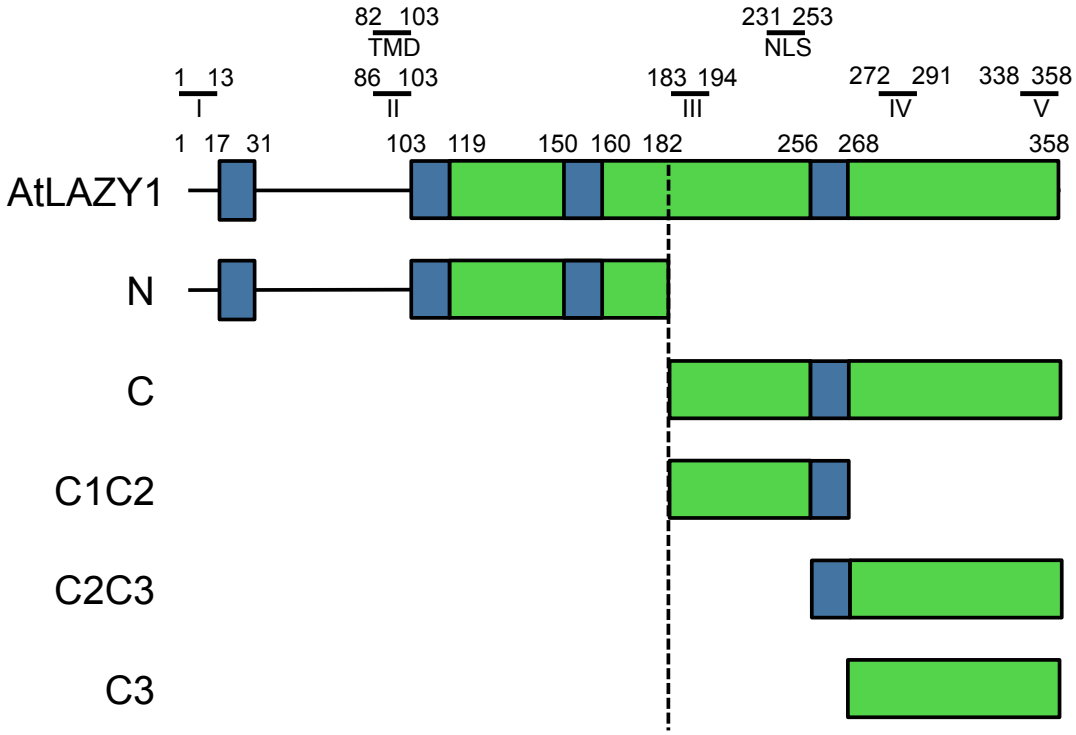


Figure 25. Schematic diagram of AtLAZY1 and its fragments used in this study. In the structural model shown at the top, potential globular and disordered domains as predicted with GlobPlot are displayed in green and blue boxes, respectively. Five short regions, I to V, which are conserved in rice and Arabidopsis LAZY1 families are also shown, as well as a putative nuclear localization signal (NLS) of AtLAZY1 (Yoshihara et al. 2013) and a transmembrane domain (TMD) predicted in rice LAZY1 (Li et al. 2007).

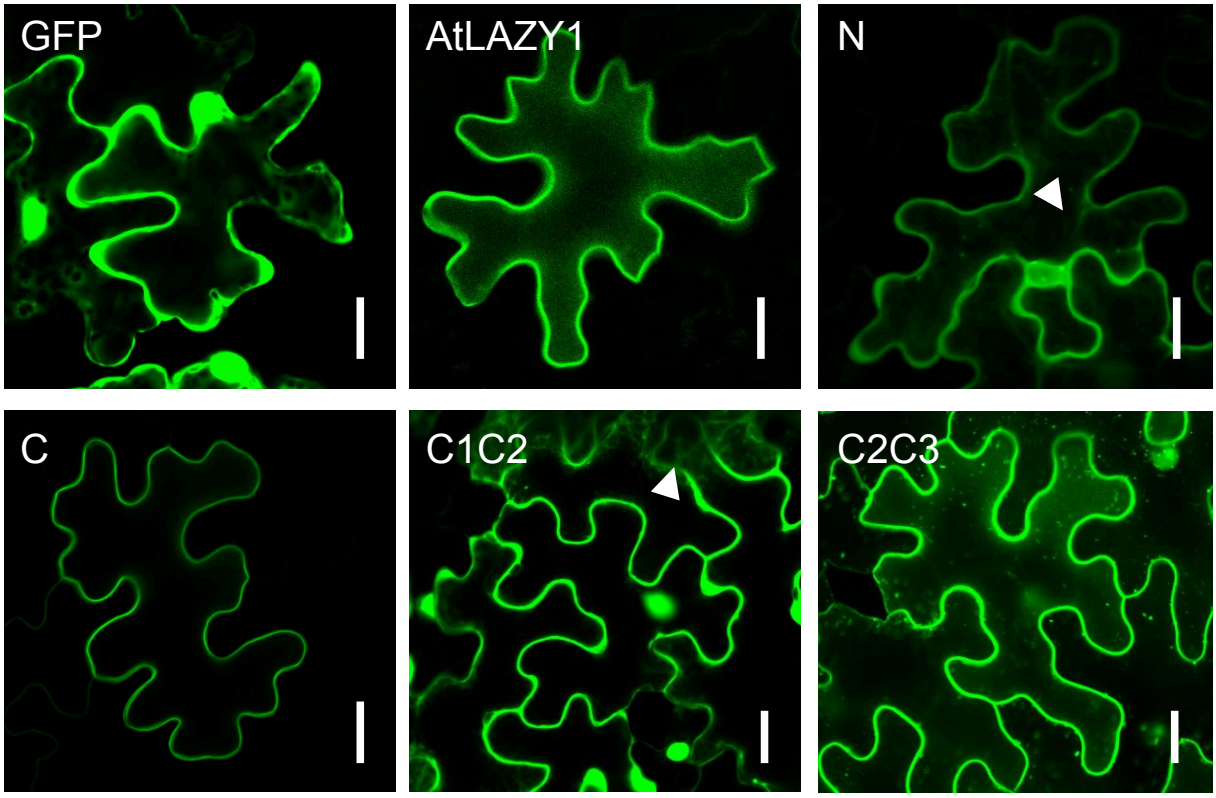


Figure 26. Fluorescent images of the pavement cells of *N. benthamiana* that transiently expressed AtLAZY1 or its truncated proteins fused to GFP by 35S promoter by using the agro-infiltration method (Kapila et al. 1997). Arrowheads indicate cytoplasmic strand. Bar = 20 μm.

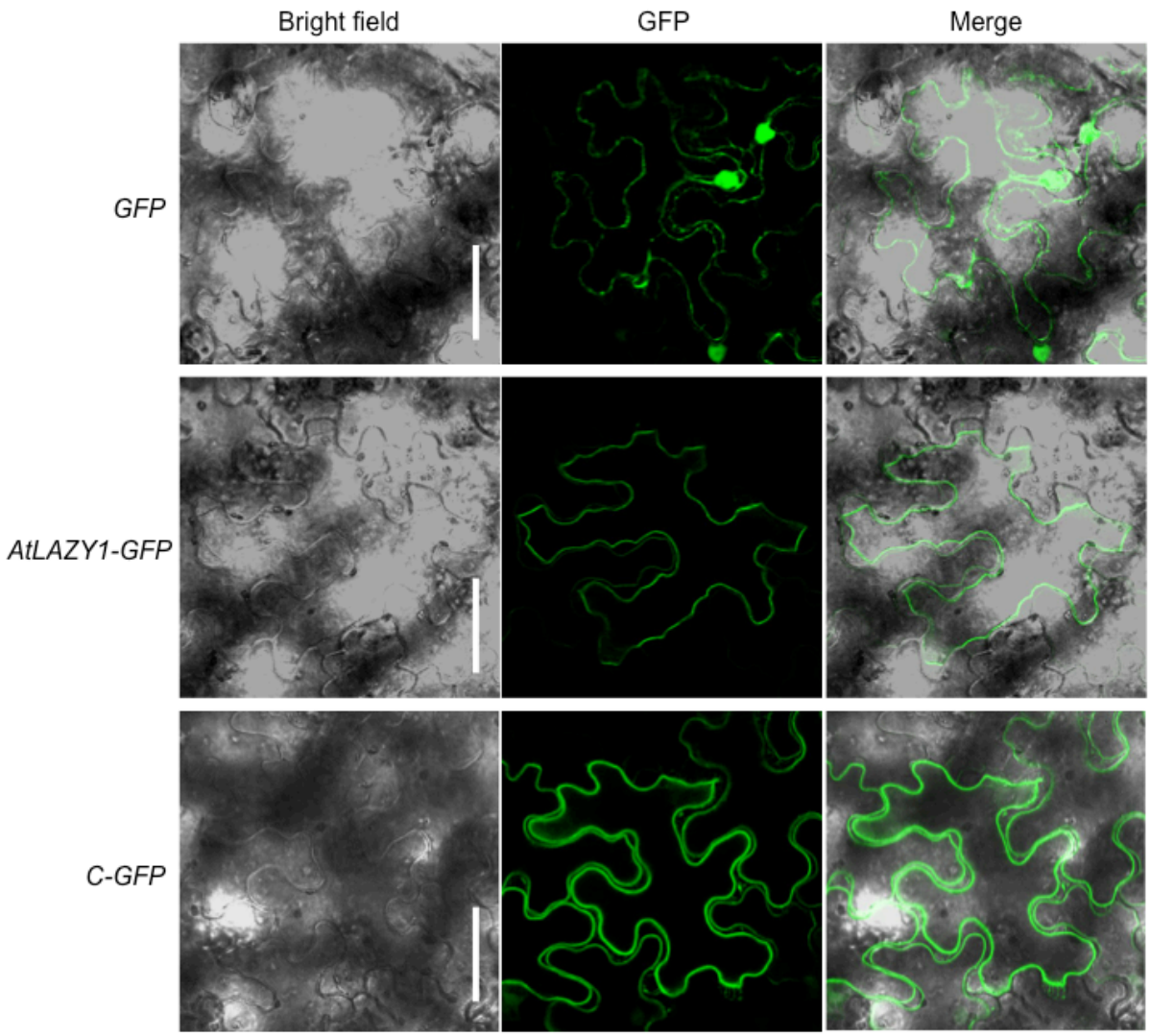


Figure 27. Plasmolysis assays of AtLAZY1-GFP and C3-GFP induced by 700 mM sucrose solution. GFP was used as a control. Each protein was transiently expressed in *N. benthamiana* pavement cells under the control of CaMV 35S promoter. Bar = 50 μm.

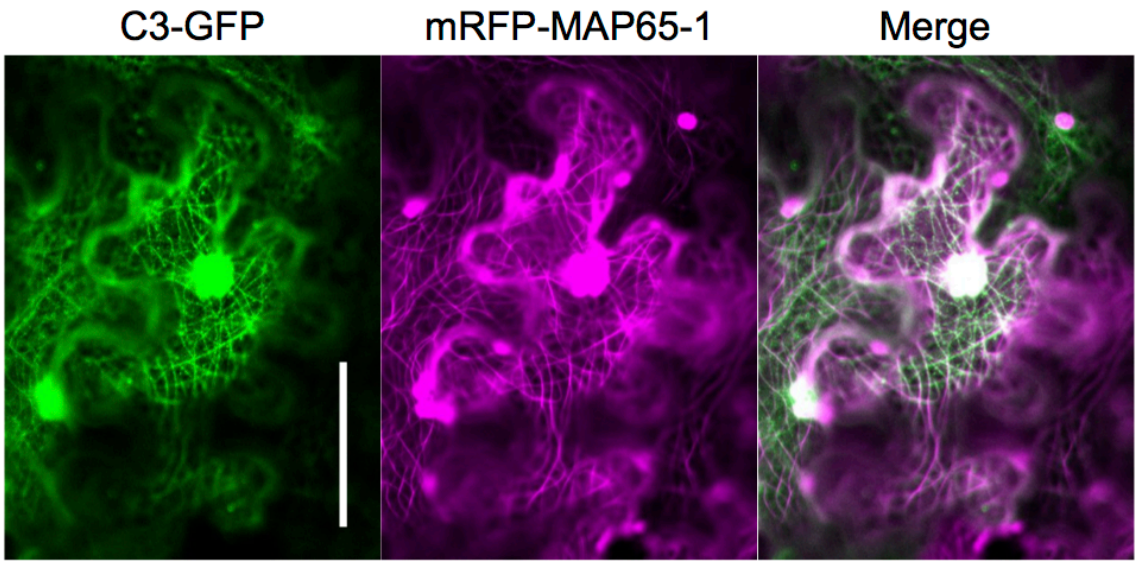


Figure 28. The C-terminal fragments of AtLAZY1 binds to microtubules. Fluorescent images of the pavement cells of *N. benthamiana* co-expressing C3-GFP and mRFP-MAP65-1. The focal plane was set on surface of the cells. White color in the merged image indicates colocalization. Bar = 50 μm.

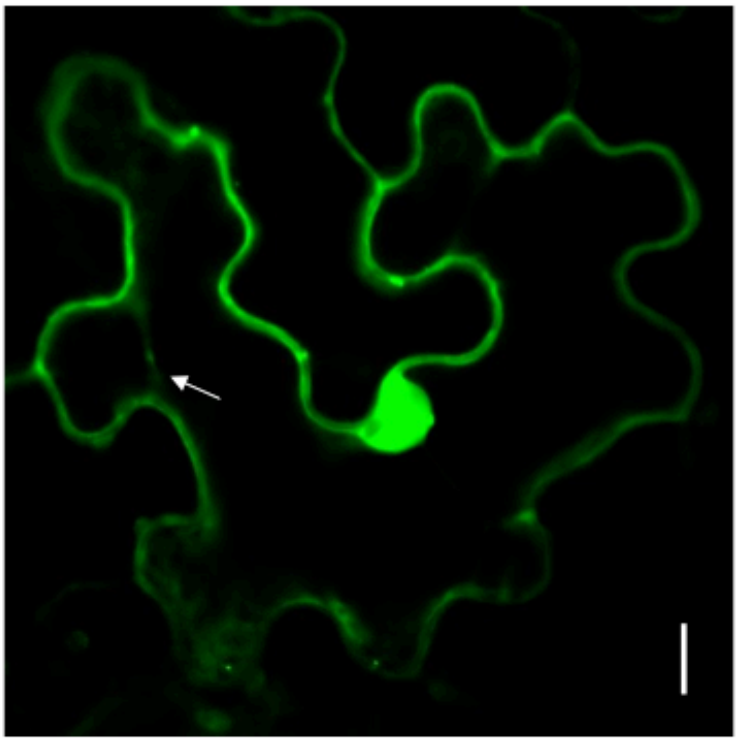


Figure 29. Fluorescent image of the pavement cells of *N. benthamiana* leaf expressing GFP fusion protein of C3. The focal plane was set on the middle of a nucleus. Arrow indicates cytoplasmic strand. Bar = 20 μm.

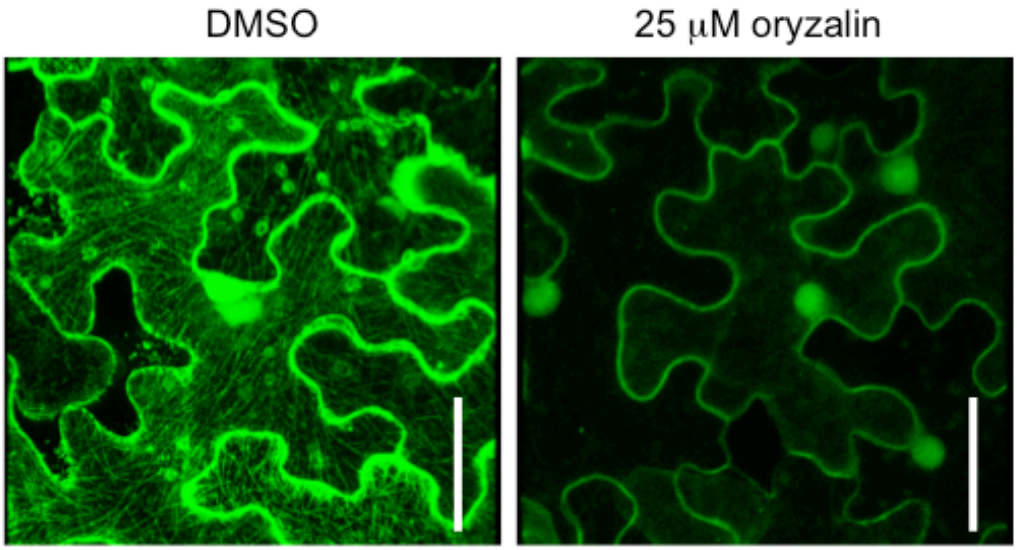


Figure 30. Stacked fluorescent images of optical sections of *N. benthamiana* pavement cells expressing GFP fusion protein of C3. Agrobacterium harboring *p35S::C3-GFP* vector was co-infiltrated with mock (DMSO) or MT-depolymerizing drug (25 μM oryzalin) and then incubated for two days. The fibrous localization pattern was abolished in the oryzalin-treated cells. Bar = 50 μm.

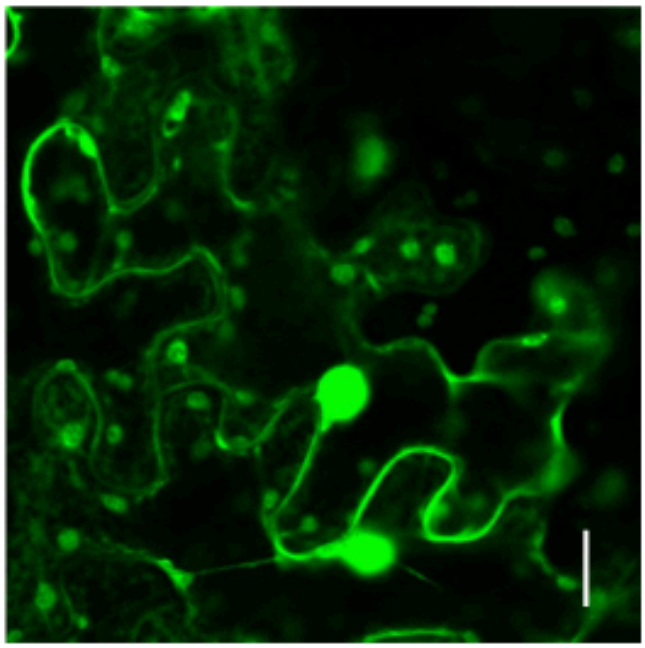


Figure 31. Fluorescent image of the pavement cells of *N. benthamiana* leaves expressing GFP fusion protein of C3 without C-terminal 48 amino acids. The fibrous localization pattern was not observed. Bar = 20 μm.

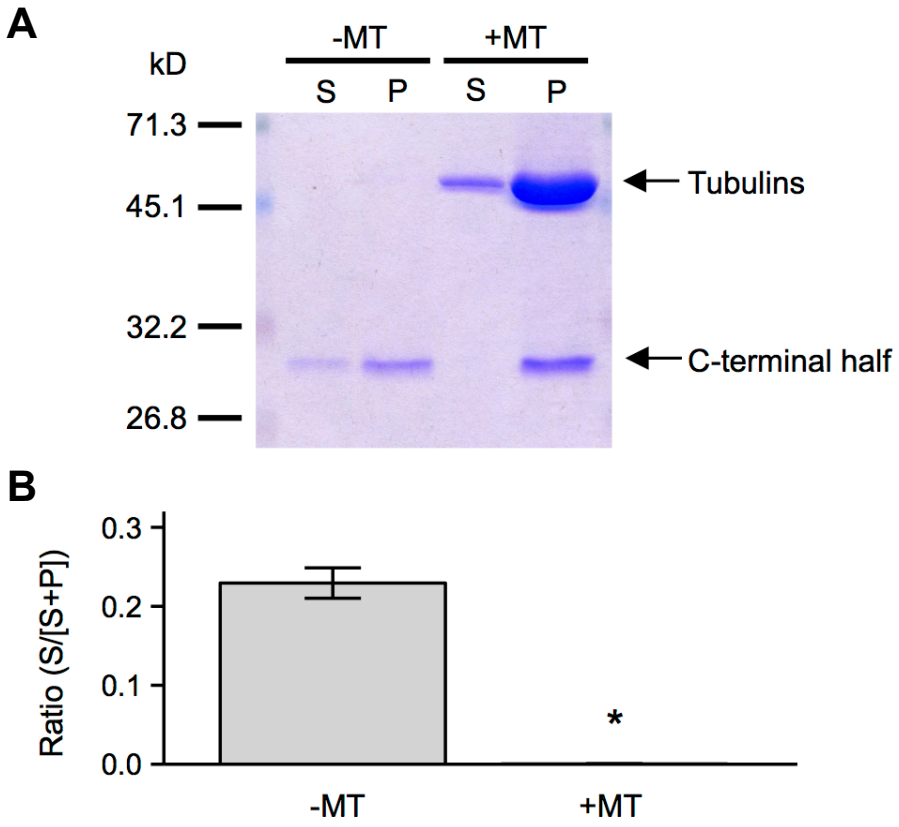


Figure 32. (A) Cosedimentation of taxol-stabilized MTs and the C-terminal half of AtLAZY1. The C-terminal half of AtLAZY1 was incubated with (+MT) or without (-MT) polymerized MTs and then centrifuged to obtain the supernatants (S) and pellets (P). They were separated on an SDS-PAGE gel and stained with Coomassie blue. (B) Quantitative examination of association of the C-terminal half with MTs. Intensities of the band of the C-terminal half in MT cosedimentation assays shown in (A) were quantitated and the ratios of the band intensities in S to those in S plus P are shown. The data represent the mean ± SD of three independent samples. Asterisk represents statistical significance between samples with or without MT ($p < 0.005$, Student's *t*-test).

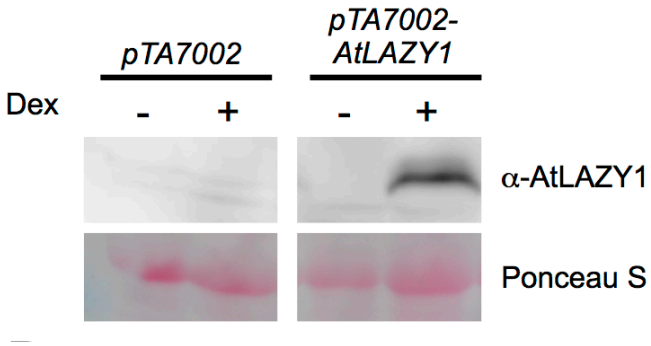


Figure 33. Immunoblot analysis of AtLAZY1 in total protein extracts from 4-day-old seedlings treated with 10 μM dex for 160 min. *pTA7002* represents an empty vector. Total proteins were subjected to immunoblot analyses after SDS-PAGE. Polyclonal anti-AtLAZY1 antibody was prepared against AtLAZY1 protein expressed and purified from *E. coli*.

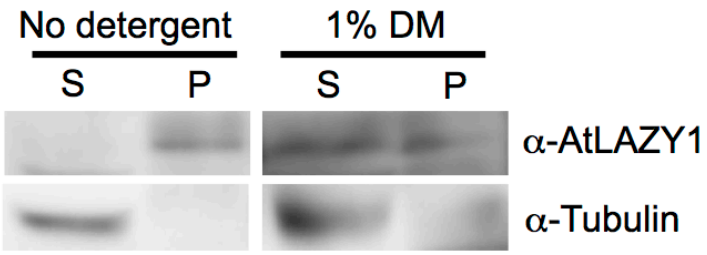


Figure 34. Effects of 1% n-dodecyl-β-D-maltoside (DM) on fractionation of AtLAZY1 and a-tubulin in cell extracts. Five 7-day-old seedlings of the transgenic plants were homogenized in 50 μl of 20 mM HEPES (pH 7.5) plus 150 mM NaCl with or without 1% DM. After incubation for 5 min on ice, the homogenates were divided into the supernatant (S) and the pellet (P) by centrifugation at 25,000*g* for 10 min. Tubulin was detected using monoclonal anti-a-tubulin antibody.

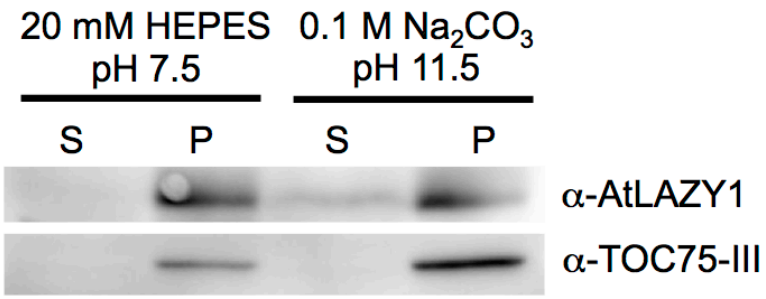


Figure 35. Effects of 0.1 M sodium bicarbonate (pH 11.5) on fractionation of AtLAZY1 and TOC75-III in cell extracts. S and P were derived after extraction with 20 mM HEPES (pH 7.5) or 0.1 M sodium bicarbonate (pH 11.5). TOC75-III was detected with anti-TOC75 antibody.